Published for SISSA by Springer

Received: *May 16, 2015*
Revised: *August 17, 2015*
Accepted: *August 25, 2015*
Published: *September 28, 2015*

Stationary black holes: large D analysis

Ryotaku Suzuki[a] **and Kentaro Tanabe**[b]

[a] *Department of Physics, Osaka City University, Osaka 558-8585, Japan*

[b] *Theory Center, Institute of Particles and Nuclear Studies, KEK, Tsukuba, Ibaraki, 305-0801, Japan*

E-mail: ryotaku@sci.osaka-cu.ac.jp, ktanabe@post.kek.jp

Abstract: We consider the effective theory of large D stationary black holes. By solving the Einstein equations with a cosmological constant using the $1/D$ expansion in near zone of the black hole we obtain the effective equation for the stationary black hole. The effective equation describes the Myers-Perry black hole, bumpy black holes and, possibly, the black ring solution as its solutions. In this effective theory the black hole is represented as an embedded membrane in the background, e.g., Minkowski or Anti-de Sitter spacetime and its mean curvature is given by the surface gravity redshifted by the background gravitational field and the local Lorentz boost. The local Lorentz boost property of the effective equation is observed also in the metric itself. In fact we show that the leading order metric of the Einstein equation in the $1/D$ expansion is generically regarded as a Lorentz boosted Schwarzschild black hole. We apply this Lorentz boost property of the stationary black hole solution to solve perturbation equations. As a result we obtain an analytic formula for quasinormal modes of the singly rotating Myers-Perry black hole in the $1/D$ expansion.

Keywords: Classical Theories of Gravity, Black Holes

ArXiv ePrint: 1505.01282

doi:10.1007/JHEP09(2015)193

JHEP09(2015)193

Contents

1 Introduction

The infinite dimensional limit of General Relativity gives not only various interesting pictures of black hole physics, but also new useful analytic method to solve gravitational problem [1–10]. The perturbation problem, such as quasinormal modes (QNMs), has been solved for general static black holes [7, 8] and the Myers-Perry black hole with equal spin [6]. As for non-linear problem the effective theory for the large D black hole has been considered recently in [9, 10] and some non-trivial static solutions were constructed. In this paper

JHEP09(2015)193

we study the effective theory of the large D stationary black hole in asymptotically flat or Anti-de Sitter (AdS) background.

The reason for the simplification of the gravity at large D is simple [2]. The radial gradient of the gravitational field around black holes becomes very large with $O(D/r_0)$ at large D. r_0 is the black hole size. So the tangential dynamics along the horizon becomes sub-dominant, and the system reduces to the ordinarily differential equation system with respect to the radial direction. In addition the appearance of the hierarchical sale, r_0/D and r_0, gives two separated excitations around the black hole, that is, the non-decoupled mode with the frequency $\omega r_0 = O(D)$ and decoupled mode $\omega r_0 = O(D^0)$. While the non-decoupled mode is universal for black holes [5], the decoupled mode has a particular and interesting feature for each black hole. For instance the instability of the ultraspinning back holes and black branes are belonging to this decoupled sector [2, 6]. These two facts, the dominance of the radial dynamics and appearance of two hierarchical scales, make General Relativity simple and analytically solvable, but still non-trivial at large D.

Achievements in QNMs by large D method motivate us to construct the effective theory for general black hole solutions in the $1/D$ expansion as a next step. The gravitational field of the black hole is localized in the near region of the horizon due to its large gradient at $D \to \infty$. Then the black hole can be regarded as a membrane Σ_B in the background spacetime like the membrane paradigm [11–13] at this limit. The physical feature of Σ_B is determined by solving Einstein equations in near zone of the black hole. If we consider the decoupled mode dynamics of the black hole, the Einstein equations can be solved consistently only in near zone. The obtained solution gives the boundary condition for Σ_B as physical properties. Then we can construct the effective theory of the large D black hole as the membrane Σ_B in the background spacetime. This construction of the effective theory has been considered in [9] for static black holes and for more general solutions with time dependences in [10].

Here we study the effective theory for general large D stationary black holes in the Minkowski or AdS background such as the (AdS)Myers-Perry black hole, bumpy black holes and black ring. These solutions have been known as exact solutions [14–16] or numerical solutions [17–19]. We obtain the general analytic metric for the stationary black holes in the $1/D$ expansion, which describes these solutions in the unified manner. The solution gives the equation for the embedding of Σ_B in the background. This embedding determines the horizon topology and its geometric shape. Then the effective equation for the embedding of Σ_B is given by the equation for the mean curvature K of Σ_B as

$$\gamma^{-1} K\Big|_{\Sigma_B} = 2\kappa, \tag{1.1}$$

where γ is a redshift factor containing both the gravitational redshift on the membrane from the background geometry and the Lorentz redshift from the local rotation along the membrane, i.e.,

$$\gamma^{-1} = \sqrt{-g_{tt}(1 - \Omega_H^2 \mathcal{R}_\phi^2)}. \tag{1.2}$$

κ and Ω_H are the surface gravity and horizon angular velocity of the black hole respectively.

JHEP09(2015)193

$\mathcal{R}_\phi$ is the rotation radius of Σ_B defined by

$$\mathcal{R}_\phi = \sqrt{-\frac{g_{\phi\phi}}{g_{tt}}}\Bigg|_{\Sigma_B}. \tag{1.3}$$

A solution of this effective equation gives the black hole metric which solves the leading order Einstein equation in the $1/D$ expansion. This effective equation is one of main results of this paper. In the static case this effective equation reduces to one of static black holes [9].

The effective equation implies that the mean curvature of Σ_B is regarded as the surface gravity redshifted by the local Lorentz boost. This local Lorentz boost property of the effective equation turns out to be also the property of the leading order metric itself. Actually we find that the leading order metric in near zone is obtained as a Lorentz boosted Schwarzschild black hole. This property of the leading order solution would not hold if we go to the higher order structure in the $1/D$ expansion. However it can still play a crucial role in solving the Einstein equations. As one interesting example, we show that perturbation equations on the obtained leading order general stationary black hole can be explicitly solved by using the solution of one of the Schwarzschild black hole. This perturbation solution, of course, contains the solution of perturbation equations of the Myers-Perry black hole. Going to the higher order of perturbation equations in the $1/D$ expansion we obtain an analytic formula for QNMs frequency of the singly rotating Myers-Perry black hole both for the axisymmetric and non-axisymmetric perturbations. As a result the threshold angular momentum of the ultraspinning instability of the singly rotating Myers-Perry black hole is found to be

$$\frac{a^2}{r_0^2} = 2k_S - 1, \qquad k_S = 1, 2, 3, \ldots \tag{1.4}$$

where r_0 is the horizon radius and k_S is a positive integer. This result can be obtained in a much easier and simpler manner by examining the effective equation (1.1) for the embedding of the bumpy black hole. Note that there is no dynamical instability at the threshold angular momentum of the case $k_S = 1$. The threshold for $k_S = 1$ does not imply any existence of a bifurcation zero-mode. There is only a trivial perturbation along the Myers-Perry solution branch.

The remaining of this paper is organized as follows. In section 2 we consider the effective theory for stationary black holes at large D. We give the leading order solution and its boost representation. The effective equation for the large D stationary black holes is derived from this leading order metric. We study a simple solution and non-trivial solutions of the effective equation there. In section 3 we apply the boost property of the leading order solution to solve perturbation equations on the general stationary solutions. The section 4 pursues the consideration for the perturbation in the previous section in more detail. We concentrate on the perturbation of the Myers-Perry black hole and obtain the QNMs frequency analytically. We close this paper by discussion and outlook in section 5. The appendices contain some technical details of calculations for the main part.

JHEP09(2015)193

2 Large D stationary black holes

We study the D dimensional stationary black hole solution and its large D effective theory. The following analysis is performed in the similar way with static case [9].[1] We use the small expansion parameter $1/n$ where

$$n = D - 3, \tag{2.1}$$

instead of $1/D$.

2.1 Set up

The large D black hole has a very large gradient along the radial direction, ρ, with $O(n)$. Then our metric ansatz for the D dimensional stationary black hole is given by

$$ds^2 = \frac{N(\rho,z)^2}{n^2} d\rho^2 + g_{ab} dx^a dx^b. \tag{2.2}$$

z is one of $D-1$ dimensional coordinate x^a. In this paper we consider the metric which has only one inhomogeneous coordinate, z, other than ρ for simplicity. The generalization to several inhomogeneous coordinate case would be straightforward as done in [9]. Then the Einstein equation with a cosmological constant

$$\Lambda = -\frac{(D-1)(D-2)}{L^2} \tag{2.3}$$

is decomposed on $\rho =$ constant surface to

$$-R + K^2 - K^a{}_b K^b{}_a - \frac{(D-1)(D-2)}{L^2} = 0, \tag{2.4}$$

$$\nabla_a K^a{}_b - \nabla_b K = 0, \tag{2.5}$$

$$\frac{n}{N}\partial_\rho K^a{}_b = -K K^a{}_b + R^a{}_b + \frac{D-1}{L^2}\delta^a{}_b - \frac{1}{N}\nabla^a \nabla_b N, \tag{2.6}$$

and

$$K^a{}_b = \frac{n}{2N(\rho,z)} g^{ac} \partial_\rho g_{cb}\,. \tag{2.7}$$

R_{ab} and ∇_a is the Ricci curvature and covariant derivative of $D-1$ dimensional metric g_{ab} respectively. K_{ab} is the extrinsic curvature of $D-1$ dimensional $\rho =$ constant surface.

We consider stationary solutions with a rotation. Then the $D-1$ dimensional metric ansatz for g_{ab} is

$$\begin{aligned} ds^2_{D-1} &= g_{ab} dx^a dx^b \\ &= -A(\rho,z)^2 dt^2 + F(\rho,z)^2 (d\phi - W(\rho,z) dt)^2 \\ &\quad + G(\rho,z)^2 dz^2 + H(\rho,z)^2 q_{AB} dx^A dx^B, \end{aligned} \tag{2.8}$$

where x^A and q_{AB} are a coordinate and the standard metric on S^{D-4} respectively. We solve the Einstein equations for K_{ab} and metric functions $A(\rho,z)$, $F(\rho,z)$, $W(\rho,z)$, $G(\rho,z)$ and $H(\rho,z)$ by using the $1/D$ expansion. In the following we specify large D behaviors of these functions and boundary conditions as a set up.

[1] But the index notation is changed from [9] .

JHEP09(2015)193

Large D behavior. At first each metric functions should be $O(n^0)$. In particular

$$g_{zz} = O(n^0) \tag{2.9}$$

implies that the derivative with respect to z is $O(n^0)$. The hierarchical scaling between $\rho-$ and $z-$ dependence makes the leading order equation at $D \to \infty$ be ordinary differential equations with respect to ρ. Next we assume that the leading order of $G(\rho, z)$ and $H(\rho, z)$ has only z-dependence and no ρ-dependence. This assumption is motivated by the exact solution of the Myers-Perry black hole (see appendix A) and the fact that the large dimensionality of the sphere gives another D factor in ρ-dependent terms through the trace on S^{D-4}. Thus we assume

$$K^z{}_z, K^A{}_B = O(n^0), \tag{2.10}$$

while the leading order of $A(\rho, z)$, $F(\rho, z)$ and $W(\rho, z)$ has ρ-dependences as

$$K^t{}_t, K^t{}_\phi, K^\phi{}_\phi, K = O(n). \tag{2.11}$$

From these assumptions we can derive the scaling law of various geometric quantities at large D. For example, the Ricci scalar R of g_{ab} is $O(n^2)$.

Boundary condition. The boundary conditions are imposed on the horizon and at the asymptotic infinity of near zone defined by $n \gg \rho \gg 1$.[2] At the horizon the extrinsic curvature has a singular behavior essentially only in one component. This condition guarantees the regularity of following quantities

$$K - K^t{}_t - K^\phi{}_\phi, \quad K^z{}_z, \quad K^A{}_B, \tag{2.12}$$

on the horizon. For the static case $K^\phi{}_\phi$ should be regular on the horizon. In this paper we consider the asymptotically flat or AdS black hole. Then the boundary condition at asymptotic infinity of near zone is

$$A(\rho, z) = \mathsf{V}_0(z) + O(1/n, e^{-2\rho}), \quad W(\rho, z) = O(e^{-2\rho}). \tag{2.13}$$

Note that the Newton potential of the black hole is $O(e^{-2\rho})$ in our gauge. So this asymptotic boundary condition means the leading order metric becomes the flat or AdS metric other than the potential term at $\rho \gg 1$. While $g_{t\phi}$ should be damping exponentially in ρ at all order of $1/D$, g_{tt} has some terms which does not decay at the asymptotic infinity in the higher order solution in the $1/D$ expansion when we consider the asymptotically AdS case (See appendix A). Since we solve the leading order equations in this section, we do not explore this structure in detail. The boundary condition (2.13) is enough for the leading order solutions.

[2] The effective theory of the large D black holes is described as the membrane physics seen from the far zone [9]. In the overlap zone $n \gg \rho \gg 1$ we can obtain physical properties of the membrane by the near zone solution as the boundary condition.

JHEP09(2015)193

2.2 Solving the leading order equation

We solve the leading order equation of the Einstein equation in the $1/D$ expansion by performing ρ integrations. This integration gives free functions of z as integration functions. They consist of the effective theory of large D stationary black holes.

Our large D scaling assumptions give following large D behaviors

$$N(\rho, z) = N_0(z) + O(1/n), \tag{2.14}$$
$$G(\rho, z) = 1 + O(1/n), \tag{2.15}$$
$$H(\rho, z) = \mathcal{R}_{\rm H}(z) + O(1/n), \tag{2.16}$$

where ρ-dependence of the leading order of $N(\rho, z)$ and z-dependence of the leading order of $G(\rho, z)$ have been absorbed into the definition of ρ and z coordinate respectively. The leading order of the Ricci scalar of g_{ab} can be calculated from this ansatz as

$$R = n^2 \left(\frac{1}{L^2} + \frac{1}{\mathcal{R}_{\rm H}(z)^2} - \frac{\mathcal{R}'_{\rm H}(z)^2}{\mathcal{R}_{\rm H}(z)^2} \right), \tag{2.17}$$

where here and in the following we omit $O(1/n)$ symbols showing the existence of subleading corrections in $1/D$ for the simplicity in the representation. Then the trace part of eq. (2.6) is integrated to

$$K = \frac{n}{r_0(z)} \coth \left(\frac{N_0(z)}{r_0(z)} (\rho - \rho_0(z)) \right), \tag{2.18}$$

where we defined $r_0(z)$ by

$$\frac{1}{r_0(z)^2} = \frac{1}{L^2} + \frac{1}{\mathcal{R}_{\rm H}(z)^2} - \frac{\mathcal{R}'_{\rm H}(z)^2}{\mathcal{R}_{\rm H}(z)^2}. \tag{2.19}$$

$\rho_0(z)$ is the horizon position $\rho = \rho_0(z)$, so we can set to $\rho_0(z) = 0$ by a gauge choice. The residual gauge in ρ coordinate can be used to have

$$N_0(z) = 2 r_0(z). \tag{2.20}$$

Note that this choice for $N_0(z)$ is different from [9] by factor two. This is just a gauge choice and it does not affect physical properties. The equations for $K^t{}_t$, $K^t{}_\phi$ and $K^\phi{}_\phi$ in eq. (2.6) are solved by

$$K^t{}_t = n \frac{C_{tt}(z)}{r_0(z) \sinh 2\rho}, \quad K^t{}_\phi = n \frac{C_{t\phi}(z)}{r_0(z) \sinh 2\rho}, \quad K^\phi{}_\phi = n \frac{C_{\phi\phi}(z)}{r_0(z) \sinh 2\rho}. \tag{2.21}$$

$C_{tt}(z)$, $C_{t\phi}(z)$ and $C_{\phi\phi}(z)$ are integration functions with respect to the ρ integration. The boundary condition on the horizon (2.12) gives

$$1 - C_{tt}(z) - C_{\phi\phi}(z) = 0. \tag{2.22}$$

JHEP09(2015)193

In the following we eliminate $C_{\phi\phi}(z)$ by this condition. Then we can integrate other components of eqs. (2.6) and (2.7), and obtain the following leading order solutions

$$A(\rho,z)^2 = \frac{A_0(z)^2 F_0(z)^2 \tanh^2\rho}{F_0(z)^2 - A_0(z)^2 C_{t\phi}(z)^2 \tanh^2\rho}, \tag{2.23}$$

$$F(\rho,z)^2 = F_0(z)^2 - A_0(z) C_{t\phi}(z)^2 \tanh^2\rho, \tag{2.24}$$

$$W(\rho,z) = \frac{F_0(z)^2(1-C_{tt}(z)) - A_0(z)^2 C_{t\phi}(z)^2 C_{tt}(z)\tanh^2\rho}{C_{t\phi}(z)F_0(z)^2 - A_0(z)^2 C_{t\phi}(z)^3 \tanh^2\rho}, \tag{2.25}$$

and

$$G(\rho,z) = 1 - \frac{2r_0(z)^2}{n}\left(\frac{\mathcal{R}_{\rm H}''(z)}{\mathcal{R}_{\rm H}(z)} - \frac{1}{L^2}\right)\log(\cosh\rho), \tag{2.26}$$

$$H(\rho,z) = \mathcal{R}_{\rm H}(z)\left(1 + \frac{2}{n}\log(\cosh\rho)\right). \tag{2.27}$$

$A_0(z)$ and $F_0(z)$ are integration functions. The integration functions of $G(\rho,z)$ and $H(\rho,z)$ are absorbed into the $O(1/n)$ redefinition of z coordinate and $\mathcal{R}_{\rm H}(z)$. The scalar constraint equation (2.4) could be satisfied by choosing the integration function in $W(\rho,z)$ properly. We can see that these solutions reduce to the static solution [9] if we set to

$$C_{tt}(z) = 1, \quad C_{t\phi} = 0. \tag{2.28}$$

We could solve the scalar constraint equation (2.4) and all evolution equations of eqs. (2.6) and (2.7). The remaining equation is the vector constraint equation (2.5). The vector constraint equation gives an additional condition between integration functions as

$$\frac{d}{dz}\log\left(\frac{A_0(z)C_{tt}(z)}{r_0(z)}\right) - (1-C_{tt}(z))\frac{d}{dz}\log\left(\frac{C_{tt}(z)}{C_{t\phi}(z)}\right) = 0\,. \tag{2.29}$$

This equation, at first glance, seems to be a non-trivial condition. However we can make this equation trivial in the following sense. To realize this we observe the surface gravity κ and angular velocity Ω_H of the horizon of the leading order solution. These quantities are read as

$$\kappa = \frac{n}{2}\frac{A_0(z)}{r_0(z)}, \qquad \Omega_H = \frac{1-C_{tt}(z)}{C_{t\phi}(z)}. \tag{2.30}$$

These quantities should be constant on the horizon [20]. Then, using the condition that κ and Ω_H are constant, we can see that the constraint equation (2.29) is satisfied automatically. Thus the vector constraint equation becomes trivial under the constancy condition of the surface gravity and angular velocity of the horizon. This is the same situation with the static case [9]. In the static case the vector constraint is equivalent to the constancy condition of the surface gravity. In stationary case the vector constraint can be satisfied if we use the constancy condition of not only the surface gravity but also the horizon angular velocity. One may feel that this statement is strange since originally the constancy of the surface gravity and angular velocity of the horizon was shown by using the Einstein equations [20]. It means that the constancy condition of the surface gravity and horizon angular

JHEP09(2015)193

velocity should be derived conditions, not additionally imposed one to satisfy the Einstein equation. In fact the constancy conditions (2.30) can be derived if we use eq. (2.29) and another equation which is obtained at the next-to-leading order of $1/D$ expansions. The regularity condition of the next-to-leading order correction of $K^z{}_z$ on the horizon requires one additional condition between $A_0(z)$ and $F_0(z)$ (see eq. (B.17)). Then these two equations give the constancy condition of the surface gravity and horizon angular velocity as eq. (2.30). The detail of this argument will be given in the appendix B. So, here, we assume the constancy conditions (2.30) on the leading order solution in advance. If constancy conditions (2.30) are not satisfied, the next-to-leading order solutions becomes singular at the horizon although the leading order solutions still regular. So we can replace $A_0(z)$ and $C_{t\phi}(z)$ by $C_{tt}(z)$, κ and $\Omega_{\rm H}$ using eq. (2.30).

Finally we impose the boundary condition at the asymptotic infinity (2.13) on the leading order solutions. Then we find

$$C_{tt}(z) = \frac{\mathsf{V}_0(z)^2}{4\hat{\kappa}^2 r_0(z)^2}, \qquad F_0(z)^2 = \frac{\mathsf{V}_0(z)^2 - 4\hat{\kappa}^2 r_0(z)^2}{4\hat{\kappa}^2 \Omega_H^2 r_0(z)^2}, \tag{2.31}$$

where we defined the reduced surface gravity $\hat{\kappa}$ by

$$\kappa = n\hat{\kappa}. \tag{2.32}$$

As a result we obtain regular leading order solutions as

$$A(\rho,z)^2 = \frac{4\hat{\kappa}^2 r_0(z)^2 \mathsf{V}_0(z)^2 \sinh^2\rho}{\mathsf{V}_0(z)^2 + 4\hat{\kappa}^2 r_0(z)^2 \sinh^2\rho}, \tag{2.33}$$

$$F(\rho,z)^2 = (\mathsf{V}_0(z)^2 - 4\hat{\kappa}^2 r_0(z)^2)\ \frac{\mathsf{V}_0(z)^2 + 4\hat{\kappa}^2 r_0(z)^2 \sinh^2\rho}{4\Omega_H^2 \hat{\kappa}^2 r_0(z)^2 \cosh^2\rho}, \tag{2.34}$$

$$W(\rho,z) = \frac{\Omega_H}{\mathsf{V}_0(z)^2 + 4\hat{\kappa}^2 r_0(z)^2 \sinh^2\rho}, \tag{2.35}$$

and eqs. (2.26) and (2.27) for $G(\rho,z)$ and $H(\rho,z)$. One can check that the (AdS)Myers-Perry black hole is described by this leading order solution as seen in appendix A.

2.3 Effective equation

In the same spirit with [9] we can obtain the effective equation for the stationary black hole from the leading order solution of near zone obtained above. The near zone metric is matched with the far zone metric at overlap zone $n \gg \rho \gg 1$ under the boundary condition (2.13). The near zone metric on $\rho =$ constant surface Σ_B at overlap zone is

$$ds^2|_{\Sigma_B} = -\mathsf{V}_0(z)^2 dt^2 + \frac{\mathsf{V}_0(z)^2 - 4\hat{\kappa}^2 r_0(z)^2}{\Omega_H^2} d\phi^2 + dz^2 + \mathcal{R}_{\rm H}(z)^2 q_{AB} dx^A dx^B, \tag{2.36}$$

where we neglect the potential terms $O(e^{-2\rho})$. Notice that the trace of the extrinsic curvature, K, is read as

$$K\Big|_{\Sigma_B} = \frac{n}{r_0(z)}, \tag{2.37}$$

JHEP09(2015)193

where $r_0(z)$ is given in eq. (2.19). The gravitational redshift factor of Σ_B by the background spacetime, g_{tt}, is

$$\sqrt{-g_{tt}}|_{\Sigma_B} = \mathsf{V}_0(z). \tag{2.38}$$

Using eqs. (2.37) and (2.38), we can see that the leading order solution in near zone gives the following embedding equation for Σ_B at overlap zone as

$$\sqrt{-g_{tt}(1-\Omega_H^2\mathcal{R}_\phi^2)}\; K\Big|_{\Sigma_B} = 2\kappa, \tag{2.39}$$

where we defined the rotational radius $\mathcal{R}_\phi$ by

$$\mathcal{R}_\phi = \sqrt{-\frac{g_{\phi\phi}}{g_{tt}}}\;\Bigg|_{\Sigma_B}. \tag{2.40}$$

The effective equation (2.39) gives the mean curvature of Σ_B as the surface gravity redshifted by the gravitational effect and the local Lorentz boost effect with the boost velocity v_ϕ defined by

$$v_\phi = \Omega_H \mathcal{R}_\phi. \tag{2.41}$$

The regular leading order solution contains arbitrary functions, $\mathsf{V}_0(z)$ and $\mathcal{R}_{\rm H}(z)$. These functions can be determined by specifying the embedding into the background. If one consider the embedding into the Minkowski background, we have $\mathsf{V}_0(z) = 1$ and there is only one remaining function $\mathcal{R}_{\rm H}(z)$ which should satisfy eq. (2.39). On the other hand, if one considers the embedding into AdS background, the embedding would give a non-trivial redshift factor $\mathsf{V}_0(z)$ of Σ_B. Thus the embedding into the AdS background should satisfy eqs. (2.38) and (2.39) for $\mathsf{V}_0(z)$ and $\mathcal{R}_{\rm H}(z)$.

The effective equation (2.39) for the stationary black hole can be still interpreted by a soap-film equation as one for the static case [9].[3] The membrane (soap-film) between two fluids satisfies the following equation for the mean curvature K of the membrane (see eq. (2.15) in [21])

$$K = \frac{\gamma T \Delta s - \Delta\rho}{\sigma}, \tag{2.42}$$

where σ is the surface tension, T is the temperature, Δs and $\Delta\rho$ are the differences between the entropy density and the energy density of the fluids at both sides of the membrane. γ is the same redshift factor as in eq. (1.2): in eq. (2.14) in [21], one just has to extract $\xi^2 = -g_{tt}$. If we now consider a case in which $\Delta\rho$ is negligible, then the equation (2.42) becomes

$$\gamma^{-1} K = \frac{T\Delta s}{\sigma}, \tag{2.43}$$

so if we identify $2\kappa = T\Delta s/\sigma$, then this is the same as eq. (2.39) (of course in this identification T, Δs, and σ are not independently determined, instead only their combination into κ is fixed).

[3] This interpretation of the effective equation (2.39) is due to Roberto Emparan. We thank him for sharing it with us.

JHEP09(2015)193

There are two remarks on the metric (2.36) at Σ_B. One is that the metric (2.36) does not need to have a component of $g_{t\phi}$. The metric (2.36) describes the background metric where the solution is embedded, and it does not need to be rotating itself although the solution is rotating. Thus the metric (2.36) does not need to have $g_{t\phi}$ component. Another remark is about the static limit. The static limit corresponds to the zero horizon angular velocity $\Omega_H = 0$. Then the metric (2.36) requires

$$\mathsf{V}_0(z)^2 = 4\hat{\kappa}^2 r_0(z)^2 \tag{2.44}$$

at the static limit. One may think that the appearance of this additional condition is curious. However one can immediately find that the condition (2.44) is nothing but the effective equation of general static solutions [9]

$$\sqrt{-g_{tt}}K\Big|_{\Sigma_B} = 2\kappa, \tag{2.45}$$

by using eqs. (2.37) and (2.38). This embedding equation can be obtained also by the static limit of eq. (2.39). So there is no appearance of new additional condition at the static limit.

The embedding in the Minkowski background has a constant redshift factor as

$$\mathsf{V}_0(z) = 1. \tag{2.46}$$

For the static embedding in this Minkowski background we have only one unique embedding by a round sphere corresponding to the Schwarzschild black hole [9, 22]. This fact is consistent with the uniqueness theorem of the static solution [23]. On the other hand, however, the embedding of the stationary solution allows various embeddings as seen below. This is due to the appearance of new degree of freedom in the horizon deformation described by $\Omega_{\rm H}\mathcal{R}_\phi$ in the effective equation.

2.3.1 Ellipsoidal embedding

As one application of the effective equation (2.39) we consider an ellipsoidal embedding in the Minkowski background. We embed the leading order solution by $r = r(\theta)$ in the Minkowski background using the ellipsoidal coordinate. The flat metric in the ellipsoidal coordinate is

$$\begin{aligned} ds^2 = -dt^2 + \frac{r^2 + a^2\cos^2\theta}{r^2 + a^2}dr^2 + (r^2 + a^2\cos^2\theta)d\theta^2 \\ + (r^2 + a^2)\sin^2\theta d\phi^2 + r^2\cos^2\theta d\Omega_{D-4}^2. \end{aligned} \tag{2.47}$$

a is a parameter describing the oblateness of the ellipsoidal. We set

$$\hat{\kappa} = \frac{1}{2}, \tag{2.48}$$

by using the normalization of near zone t-coordinate for simplicity. The relation z and θ can be seen from eqs. (2.36) and (2.47) with $r = r(\theta)$ as

$$\frac{dz}{d\theta} = \sqrt{\frac{(\mathcal{R}_{\rm H}(\theta)^2 + a^2\cos^4\theta)(\mathcal{R}_{\rm H}(\theta)^2 + (\mathcal{R}'_{\rm H}(\theta) + \tan\theta\mathcal{R}_{\rm H}(\theta))^2 + a^2\cos^2\theta)}{\cos^2\theta(\mathcal{R}_{\rm H}(\theta)^2 + a^2\cos^2\theta)}}, \tag{2.49}$$

JHEP09(2015)193

where we used the relation

$$r(\theta)\cos\theta = \mathcal{R}_{\rm H}(\theta) \tag{2.50}$$

in the leading order solution. Then the effective equation (2.39) becomes

$$\begin{aligned}
&\Omega_H^2 \tan^2\theta (a^2\cos^4\theta + \mathcal{R}_{\rm H}(\theta)^2 + \cos\theta\sin\theta\mathcal{R}_{\rm H}(\theta)\mathcal{R}'_{\rm H}(\theta))^2(a^2\cos^2\theta + \mathcal{R}_{\rm H}(\theta)^2) \\
&\quad + (\mathcal{R}_{\rm H}(\theta)^2 - 1)(a^2\cos^4\theta + \mathcal{R}_{\rm H}(\theta)^2)^2 \\
&\quad + 2\cos\theta\sin\theta\mathcal{R}_{\rm H}(\theta)\mathcal{R}'_{\rm H}(\theta)(\mathcal{R}_{\rm H}(\theta)^2 - 1)(a^2\cos^4\theta + \mathcal{R}_{\rm H}(\theta)^2) \\
&\quad + \cos^2\theta\mathcal{R}_{\rm H}(\theta)^2\mathcal{R}'_{\rm H}(\theta)^2(a^2\cos^4\theta + \mathcal{R}_{\rm H}(\theta)^2 - \sin^2\theta) = 0.
\end{aligned} \tag{2.51}$$

We solve this equation for $\mathcal{R}_{\rm H}(\theta)$ in some cases below.

Myers-Perry solution. The Myers-Perry solution is described by the embedding

$$\mathcal{R}_{\rm H}(\theta) = \cos\theta, \qquad \Omega_H = \frac{a}{1+a^2}, \tag{2.52}$$

in the ellipsoidal embedding for arbitrary a.

Bumpy black holes. The Myers-Perry black hole has marginally stable quasinormal modes $\omega = 0$ in the ultraspinning region [24–26]. The marginally stable modes suggest the existences of new deformed solution branching off the Myers-Perry solution branch. These solutions, so called bumpy black holes, have been constructed numerically in [17, 18]. Here we consider this solution by using the effective equation (2.51). To study this we perform the perturbative analysis of the effective equation (2.51) around the Myers-Perry black hole. We expand the embedding function $\mathcal{R}_{\rm H}(\theta)$ around the Myers-Perry black hole as

$$\mathcal{R}_{\rm H}(\theta) = \cos\theta\Big[1 + \hat{\mathcal{R}}(\theta)\epsilon + O\left(\epsilon^2\right)\Big], \tag{2.53}$$

where

$$\epsilon = \Omega_H - \frac{a}{1+a^2}. \tag{2.54}$$

Then, perturbing eq. (2.51) with respect to ϵ, we find the perturbative solution

$$\hat{\mathcal{R}}(\theta) = \frac{a(1+a^2)^2\sin^2\theta}{(1-a^2)(1+a^2\cos^2\theta)} + A\frac{\sin^{1+a^2}\theta}{1+a^2\cos^2\theta}, \tag{2.55}$$

where A is an integration constant describing the perturbation amplitude. The first part describes just the trivial perturbation adding the angular momentum along the Myers-Perry black hole solution branch. The second part is the non-trivial deformation of the solution into the bumpy black hole solution branch. For general a and $A \neq 0$, we have a non-analytic behavior in the solution at $\theta = 0$. The regularity of the solution at $\theta = 0$ requires[4]

$$a_c^2 = 2k - 1, \qquad k = 1, 2, 3, \ldots \tag{2.56}$$

[4]Here the regularity means that any derivatives of $\hat{\mathcal{R}}(\theta)$ should be finite at $\theta = 0$ and $\hat{\mathcal{R}}(\theta)$ be an even function around $\theta = 0$. To satisfy this requirement a should be discretized by k as given in eq. (2.56). As we can see in appendix C this regularity condition at $\theta = 0$ is equivalent to the condition for the spheroidal harmonics at large D. Furthermore this discretization parameter k corresponds to the angular momentum number ℓ.

JHEP09(2015)193

	$a_c\|_{k=1}$	$a_c\|_{k=2}$	$a_c\|_{k=3}$	$a_c\|_{k=4}$
eq. (2.56)	1	$\sqrt{3} = 1.732$	$\sqrt{5} = 2.236$	$\sqrt{7} = 2.646$
numerical ($D = 6$)	1.097	1.572	1.849	2.036
numerical ($D = 7$)	1.075	1.714	2.141	2.487
numerical ($D = 8$)	1.061	1.770	2.275	2.725
numerical ($D = 9$)	1.051	1.792	2.337	2.807
numerical ($D = 10$)	1.042	1.795	2.361	2.855
numerical ($D = 11$)	1.035	1.798	2.373	2.879

Table 1. Comparison of our analytic formula (2.56) for the threshold of the instability of the Myers-Perry black hole with numerical results in [26]. The analytic formula shows quite good agreements with numerical results within the expected error $O(1/D)$. The value of a_c for $k = 1$ by [26] has perfect agreements with eq. (2.57).

For $k = 1$, i.e., $a_c = 1$, the solution is same with the first part of eq. (2.55), so it corresponds to the Myers-Perry black hole with a different angular momentum. The value a_c for $k = 1$ is known analytically in all D by the thermodynamic argument [24] as

$$\left(\frac{a}{r_0}\right)^{D-3} = \frac{D-3}{2(D-4)}\left(\frac{D-3}{D-5}\right)^{(D-5)/2}. \tag{2.57}$$

r_0 is the horizon radius of the Myers-Perry black hole (see appendix A). At the large D limit the formula (2.57) gives same value with eq. (2.56) for $k = 1$. For $k > 1$ we have non-trivial bumpy black hole solutions by eq. (2.55). Eq. (2.56) gives the threshold angular momentum of the ultraspinning instability of the Myers-Perry black hole. In table 1 we show the comparison of eq. (2.56) with numerical results in [26]. Actually we have good agreements within the expected error $O(1/D)$. This threshold angular momentum will be reproduced also by observing the quasinormal mode frequency directly in section 4.

In appendix A we generalize the above analysis to the AdS Myers-Perry black hole. Then we obtain the threshold angular momentum for the ultraspinning instability of the AdS Myers-Perry black hole in the $1/D$ expansion.

2.4 Boost representation

One important property of the leading order solution in near zone is its local Lorentz boost representation. The effective equation (2.39) has the interpretation that the embedded surface Σ_B is the locally Lorentz boosted membrane. This local Lorentz boost property holds also for the metric itself in near zone. To see this we rewrite the (t, ϕ) part of the obtained leading order metric in near zone as

$$\begin{aligned} ds^2_{(t,\phi)} = &-\mathsf{V}_0(z)^2 dt^2 + \frac{\mathsf{V}_0(z)^2 - 4\hat{\kappa}^2 r_0(z)^2}{\Omega_H^2} d\phi^2 \\ &+ \frac{1}{4\hat{\kappa}^2 r_0(z)^2 \cosh^2\rho}\left(\mathsf{V}_0(z)^2 dt - \frac{\mathsf{V}_0(z)^2 - 4\hat{\kappa}^2 r_0^2}{\Omega_H} d\phi\right)^2. \end{aligned} \tag{2.58}$$

JHEP09(2015)193

By introducing the boost parameter $\sigma(z)$ defined by

$$\cosh\sigma(z) = \frac{\mathsf{V}_0(z)}{2\hat{\kappa} r_0(z)} \tag{2.59}$$

and new local frame dx^p by

$$dx^p(z) = \left(\mathsf{V}_0(z)dt,\ \frac{\sqrt{\mathsf{V}_0(z)^2 - 4\hat{\kappa}^2 r_0(z)^2}}{\Omega_H} d\phi\right), \tag{2.60}$$

the leading order metric is written in a very simple form as

$$ds^2 = \frac{4r_0(z)^2}{n^2}d\rho^2 + \left(\eta_{pq} + \frac{u_p u_q}{\cosh^2\rho}\right)dx^p dx^q + dz^2 + \mathcal{R}_{\rm H}(z)^2 d\Omega^2_{D-4}, \tag{2.61}$$

where η_{pq} is the flat metric on two dimensional spacetime. The fluid velocity u_p is

$$u_p dx^p = \mathsf{V}_0(z)\cosh\sigma(z)dt - \frac{\sqrt{\mathsf{V}_0(z)^2 - 4\hat{\kappa}^2 r_0(z)^2}}{\Omega_H}\sinh\sigma(z)d\phi. \tag{2.62}$$

Note that the leading order metric of the Schwarzschild black hole is (see appendix A)

$$ds^2 = \frac{4}{n^2}d\rho^2 - \tanh^2\rho\ dt^2 + dz^2 + \sin^2\theta d\phi^2 + \cos^2\theta d\Omega^2_{D-4}. \tag{2.63}$$

Thus the stationary solution can be represented as the locally boosted Schwarzschild black hole under the following boost transformation

$$dt \to \mathsf{V}_0(z)dt\cosh\sigma(z) - \frac{\sqrt{\mathsf{V}_0(z)^2 - 4\hat{\kappa}^2 r_0(z)^2}}{\Omega_H}d\phi\sinh\sigma(z), \tag{2.64}$$

$$d\phi \to \frac{\sqrt{\mathsf{V}_0(z)^2 - 4\hat{\kappa}^2 r_0(z)}}{\Omega_H}d\phi\cosh\sigma(z) - \mathsf{V}_0(z)dt\sinh\sigma(z). \tag{2.65}$$

This boost representation is known for the Myers-Perry black hole [3, 6]. However our leading order solution covers much wider class of solutions including the asymptotically AdS black holes. This boost representation is the universal feature for the large D stationary black holes under our ansatz.

The boost parameter, $\sigma(z)$, is not constant and the boost transformation is inhomogeneous in z-direction. This z-dependence also appears as the horizon radius inhomogeneity in $g_{\rho\rho}$. Thus the identification with the Schwarzschild black hole by the boost transformation is valid only locally in z-direction. However this inhomogeneity along z-direction is not so crucial since the dynamics along z-direction is sub-dominant compared with the radial dynamics. This boost transformation is the property of the radial dynamics, which is the leading order dynamics of large D black holes. The local effect by z-dependence would be introduced at the sub-leading order in $1/D$ expansion as corrections. Such z-dependent dynamics in the higher order structure of the $1/D$ expansion contains the essential effects by the rotation and horizon topology.

JHEP09(2015)193

3 Perturbation

As one interesting application of the boost property in the leading order solution we consider the perturbation problem. By using the boost transformation we can obtain the solution of the perturbation equation of the stationary black hole from one of the Schwarzschild black hole. In the following we investigate the decoupled mode perturbation, whose the frequency is $\omega = O(D^0)$ [7], of the asymptotically flat black hole given by

$$\mathsf{V}_0(z) = 1, \tag{3.1}$$

in the leading order metric in section 2. The extension to the asymptotically AdS black hole is straightforward.

3.1 Schwarzschild black hole

We study the perturbation on the Schwarzschild black hole. Next we perform the boost transformation on the perturbation solutions to obtain the perturbation solution of the stationary solution. There are various ways in the representation of the perturbation around the Schwarzschild black hole [27, 28]. Here we fix the gauge for the perturbation, $h_{\mu\nu}$, to solve the perturbation equation. Especially we use the transverse traceless gauge as

$$\hat{\nabla}^\mu h_{\mu\nu} = 0, \qquad \hat{g}^{\mu\nu} h_{\mu\nu} = 0, \tag{3.2}$$

where $\hat{\nabla}_\mu$ is the covariant derivative of the D dimensional background metric $\hat{g}_{\mu\nu}$. Then the perturbation equation becomes equivalent to the Lichnerowicz equation given by

$$\hat{\nabla}^\rho \hat{\nabla}_\rho h_{\mu\nu} + 2\hat{R}_{\mu\rho\nu\sigma} h^{\rho\sigma} = 0, \tag{3.3}$$

where $\hat{R}_{\mu\nu\rho\sigma}$ is a background Riemann tensor. The explicit components of the perturbation equation are complicate so we do not show them here. The background spacetime is the $D = n + 3$ dimensional Schwarzschild black hole given by

$$ds^2 = -f(r)^{-1} dt^2 + f(r)^{-1} dr^2 + r^2 \left(d\theta^2 + \sin^2\theta d\phi^2 + \cos^2\theta d\Omega_{D-4}^2 \right), \tag{3.4}$$

where

$$f(r) = 1 - \left(\frac{r_0}{r}\right)^n \equiv 1 - \frac{1}{\mathsf{R}}. \tag{3.5}$$

Here we introduced the new radial coordinate $\mathsf{R} = (r/r_0)^n$. This radial coordinate R is related with the radial coordinate ρ which we used in the previous section by

$$\mathsf{R} = \cosh^2\rho. \tag{3.6}$$

The perturbation is decomposed into the scalar, vector and tensor type with respect to S^{D-4} in the metric.[5] In this paper we investigate the scalar and vector type perturbation on S^{D-4}. Using the vielbein

$$e^{(0)}_{\rm Sch} = \sqrt{f(r)}dt,\ e^{(1)}_{\rm Sch} = \frac{dr}{\sqrt{f(r)}},\ e^{(2)}_{\rm Sch} = r d\theta,\ e^{(3)}_{\rm Sch} = r\sin\theta d\phi,\ e^{(A)}_{\rm Sch} = r\cos\theta \hat{e}^{(A)}, \tag{3.7}$$

[5] Note that the usual scalar, vector and tensor type perturbation of the Schwarzschild black hole is based on the decomposition on S^{D-2} [27]. Then, for example, our scalar type perturbation on S^{D-4} consists of the scalar, vector and tensor type perturbation on S^{D-2}.

JHEP09(2015)193

where $\hat{e}^{(A)}$ is a vielbein on the unit sphere S^{D-4}, the scalar type perturbation, $h^{(S)}_{\mu\nu}$, on S^{D-4} can be written by

$$h^{(S)}_{\mu\nu}dx^\mu dx^\nu = e^{-i\omega t}e^{im\phi}\Big[f^{(S)\mathrm{Sch}}_{IJ}\mathbb{Y}^{(S)}_j e^{(I)}_{\mathrm{Sch}}e^{(J)}_{\mathrm{Sch}} + f^{(S)\mathrm{Sch}}_{I}\mathsf{D}_A\mathbb{Y}^{(S)}_j e^{(I)}_{\mathrm{Sch}}e^{(A)}_{\mathrm{Sch}} + r^2\cos^2\theta(H^{(S)\mathrm{Sch}}_T\mathbb{Y}^{(S)}_j\gamma_{AB} + H^{(S)\mathrm{Sch}}_L\mathbb{Y}^{(S)j}_{AB})dx^A dx^B\Big], \tag{3.8}$$

where $I, J = 0, 1, 2, 3$. $\mathbb{Y}^{(S)}_j$ is the scalar harmonics on S^{D-4} satisfying

$$(\mathsf{D}^2 + \lambda_S)\mathbb{Y}^{(S)}_j = 0, \tag{3.9}$$

where the eigenvalue λ_S is given by

$$\lambda_S = j(j + D - 5). \tag{3.10}$$

The scalar derived tensor harmonics $\mathbb{Y}^{(S)j}_{AB}$ is defined by

$$\mathbb{Y}^{(S)j}_{AB} = \mathsf{D}_A\mathsf{D}_B\mathbb{Y}^{(S)}_j + \frac{\lambda_S}{D-4}\mathbb{Y}^{(S)}_j q_{AB}. \tag{3.11}$$

The vector type perturbation, $h^{(V)}_{\mu\nu}$, on S^{D-4} is given by

$$h^{(V)}_{\mu\nu}dx^\mu dx^\nu = e^{-i\omega t}e^{im\phi}\Big[f^{(V)\mathrm{Sch}}_I\mathbb{Y}^{(V)j}_A e^{(I)}e^{(A)} + H^{(V)}_L\mathbb{Y}^{(V)j}_{AB}e^{(A)}e^{(B)}\Big], \tag{3.12}$$

where $\mathbb{Y}^{(V)j}_A$ and $\mathbb{Y}^{(V)j}_{AB}$ are the vector harmonics on S^{D-4} defined by

$$(\mathsf{D}^2 + \lambda_V)\mathbb{Y}^{(V)j}_A = 0, \qquad \mathsf{D}^A\mathbb{Y}^{(V)j}_A = 0, \qquad \mathbb{Y}^{(V)j}_{AB} = \mathsf{D}_{(A}\mathbb{Y}^{(V)j}_{B)}, \tag{3.13}$$

with the eigenvalue λ_V given by

$$\lambda_V = j(j + D - 5) - 1. \tag{3.14}$$

The perturbation equation is a coupled PDE system for scalar and vector type perturbations. At large D the situation is changed and the perturbation equations become decoupled ODE system. We can find decoupled perturbation variables $F^{(S)\mathrm{Sch}}_{IJ}$ for the scalar type perturbation easily as

$$\begin{aligned}
&F^{(S)\mathrm{Sch}}_{00} = f^{(S)\mathrm{Sch}}_{00} + f^{(S)\mathrm{Sch}}_{11}, \quad F^{(S)\mathrm{Sch}}_{11} = f^{(S)\mathrm{Sch}}_{00} - f^{(S)\mathrm{Sch}}_{11}, \quad F^{(S)\mathrm{Sch}}_{01} = f^{(S)\mathrm{Sch}}_{01},\\
&F^{(S)\mathrm{Sch}}_{02} = f^{(S)\mathrm{Sch}}_{02}, \qquad F^{(S)\mathrm{Sch}}_{03} = f^{(S)\mathrm{Sch}}_{03}, \qquad F^{(S)\mathrm{Sch}}_{12} = f^{(S)\mathrm{Sch}}_{12}, \quad F^{(S)\mathrm{Sch}}_{13} = f^{(S)\mathrm{Sch}}_{13},\\
&F^{(S)\mathrm{Sch}}_{22} = f^{(S)\mathrm{Sch}}_{22}, \qquad F^{(S)\mathrm{Sch}}_{23} = f^{(S)\mathrm{Sch}}_{23}, \qquad F^{(S)\mathrm{Sch}}_{33} = f^{(S)\mathrm{Sch}}_{33},
\end{aligned} \tag{3.15}$$

and

$$F^{(S)\mathrm{Sch}}_I = f^{(S)\mathrm{Sch}}_I, \qquad F^{(S)\mathrm{Sch}}_{T,L} = H^{(S)\mathrm{Sch}}_{T,L}. \tag{3.16}$$

The vector type perturbation has following decoupled perturbation variables at large D

$$F^{(V)\mathrm{Sch}}_I = f^{(V)\mathrm{Sch}}_I, \qquad F^{(V)\mathrm{Sch}}_L = H^{(V)\mathrm{Sch}}_L. \tag{3.17}$$

JHEP09(2015)193

Then each decoupled perturbation variables are expanded at large D as

$$F_{ab}^{(S)\mathrm{Sch}} = \sum_{k\geq 0} \frac{{}^{(k)}F_{ab}^{(S)\mathrm{Sch}}}{n^k},\ F_{a}^{(S)\mathrm{Sch}} = \sum_{k\geq 0} \frac{{}^{(k)}F_{a}^{(S)\mathrm{Sch}}}{n^k},\ F_{T,L}^{(S)\mathrm{Sch}} = \sum_{k\geq 0} \frac{{}^{(k)}F_{T,L}^{(S)\mathrm{Sch}}}{n^k}, \tag{3.18}$$

for the scalar type perturbation and

$$F_{I}^{(V)\mathrm{Sch}} = \sum_{k\geq 0} \frac{{}^{(k)}F_{I}^{(V)\mathrm{Sch}}}{n^k},\ F_{L}^{(V)\mathrm{Sch}} = \sum_{k\geq 0} \frac{{}^{(k)}F_{L}^{(V)\mathrm{Sch}}}{n^k}, \tag{3.19}$$

for the vector type perturbation. By using transverse traceless gauge conditions we can obtain $F_{I}^{(S)\mathrm{Sch}}$, $F_{T,L}^{(S)\mathrm{Sch}}$ and $F_{L}^{(V)\mathrm{Sch}}$ from $F_{IJ}^{(S)\mathrm{Sch}}$ and $F_{I}^{(V)\mathrm{Sch}}$. Thus the equations to be solved are the equations of $F_{IJ}^{(S)\mathrm{Sch}}$ for the scalar type perturbation and $F_{I}^{(V)\mathrm{Sch}}$ for the vector type perturbation. The perturbation equations for $F_{IJ}^{(S)\mathrm{Sch}}$ are

$$\frac{\partial}{\partial \mathsf{R}}\mathsf{R}(\mathsf{R}-1)\frac{\partial}{\partial \mathsf{R}}{}^{(k)}F_{00}^{(S)\mathrm{Sch}} - \frac{{}^{(k)}F_{00}^{(S)\mathrm{Sch}}}{\mathsf{R}-1} = {}^{(k)}\mathcal{S}_{00}^{(S)}, \tag{3.20}$$

$$\frac{\partial}{\partial \mathsf{R}}\mathsf{R}(\mathsf{R}-1)\frac{\partial}{\partial \mathsf{R}}{}^{(k)}F_{01}^{(S)\mathrm{Sch}} - \frac{{}^{(k)}F_{01}^{(S)\mathrm{Sch}}}{\mathsf{R}-1} = {}^{(k)}\mathcal{S}_{01}^{(S)}, \tag{3.21}$$

$$\frac{\partial}{\partial \mathsf{R}}\mathsf{R}(\mathsf{R}-1)\frac{\partial}{\partial \mathsf{R}}{}^{(k)}F_{02}^{(S)\mathrm{Sch}} - \frac{{}^{(k)}F_{02}^{(S)\mathrm{Sch}}}{4\mathsf{R}(\mathsf{R}-1)} = {}^{(k)}\mathcal{S}_{02}^{(S)}, \tag{3.22}$$

$$\frac{\partial}{\partial \mathsf{R}}\mathsf{R}(\mathsf{R}-1)\frac{\partial}{\partial \mathsf{R}}{}^{(k)}F_{03}^{(S)\mathrm{Sch}} - \frac{{}^{(k)}F_{03}^{(S)\mathrm{Sch}}}{4\mathsf{R}(\mathsf{R}-1)} = {}^{(k)}\mathcal{S}_{03}^{(S)}, \tag{3.23}$$

$$\frac{\partial}{\partial \mathsf{R}}\mathsf{R}(\mathsf{R}-1)\frac{\partial}{\partial \mathsf{R}}{}^{(k)}F_{11}^{(S)\mathrm{Sch}} - \frac{{}^{(k)}F_{11}^{(S)\mathrm{Sch}}}{\mathsf{R}} = {}^{(k)}\mathcal{S}_{11}^{(S)}, \tag{3.24}$$

$$\frac{\partial}{\partial \mathsf{R}}\mathsf{R}(\mathsf{R}-1)\frac{\partial}{\partial \mathsf{R}}{}^{(k)}F_{12}^{(S)\mathrm{Sch}} - \frac{{}^{(k)}F_{12}^{(S)\mathrm{Sch}}}{4\mathsf{R}(\mathsf{R}-1)} = {}^{(k)}\mathcal{S}_{12}^{(S)}, \tag{3.25}$$

$$\frac{\partial}{\partial \mathsf{R}}\mathsf{R}(\mathsf{R}-1)\frac{\partial}{\partial \mathsf{R}}{}^{(k)}F_{13}^{(S)\mathrm{Sch}} - \frac{{}^{(k)}F_{13}^{(S)\mathrm{Sch}}}{4\mathsf{R}(\mathsf{R}-1)} = {}^{(k)}\mathcal{S}_{13}^{(S)}, \tag{3.26}$$

$$\frac{\partial}{\partial \mathsf{R}}\mathsf{R}(\mathsf{R}-1)\frac{\partial}{\partial \mathsf{R}}{}^{(k)}F_{22}^{(S)\mathrm{Sch}} = {}^{(k)}\mathcal{S}_{22}^{(S)}, \tag{3.27}$$

$$\frac{\partial}{\partial \mathsf{R}}\mathsf{R}(\mathsf{R}-1)\frac{\partial}{\partial \mathsf{R}}{}^{(k)}F_{23}^{(S)\mathrm{Sch}} = {}^{(k)}\mathcal{S}_{23}^{(S)}, \tag{3.28}$$

$$\frac{\partial}{\partial \mathsf{R}}\mathsf{R}(\mathsf{R}-1)\frac{\partial}{\partial \mathsf{R}}{}^{(k)}F_{33}^{(S)\mathrm{Sch}} = {}^{(k)}\mathcal{S}_{33}^{(S)}. \tag{3.29}$$

The $k-$th order source term ${}^{(k)}\mathcal{S}_{ab}^{(S)}$ is coming from the lower order solutions and the source term does not have the decoupling property. The perturbation variables, ${}^{(k)}F_{IJ}^{(S)\mathrm{Sch}}$, depend on R and θ.[6] However the perturbation equation becomes ordinarily differential equation with respect to R at large D. Furthermore each k-th order variables ${}^{(k)}F_{IJ}^{(S)\mathrm{Sch}}$ are decoupling and we can solve the solution by the straightforward integration procedure

[6]The Schwarzschild black hole has a spherical symmetry. So the perturbation equation can be reduced to the ordinarily differential equation in principle. Here, for the usefulness in the following discussion, we use the harmonics on S^{D-4} and the perturbation equation becomes the apparent partial differential equation.

JHEP09(2015)193

at each order. The vector type perturbation has the same property. The perturbation equation for $F_I^{(V)\mathrm{Sch}}$ is

$$\frac{\partial}{\partial \mathsf{R}}\mathsf{R}(\mathsf{R}-1)\frac{\partial}{\partial \mathsf{R}}{}^{(k)}F_0^{(V)\mathrm{Sch}} - \frac{{}^{(k)}F_0^{(V)\mathrm{Sch}}}{4\mathsf{R}(\mathsf{R}-1)} = {}^{(k)}\mathcal{S}_0^{(V)}, \tag{3.30}$$

$$\frac{\partial}{\partial \mathsf{R}}\mathsf{R}(\mathsf{R}-1)\frac{\partial}{\partial \mathsf{R}}{}^{(k)}F_1^{(V)\mathrm{Sch}} - \frac{{}^{(k)}F_1^{(V)\mathrm{Sch}}}{4\mathsf{R}(\mathsf{R}-1)} = {}^{(k)}\mathcal{S}_1^{(V)}, \tag{3.31}$$

$$\frac{\partial}{\partial \mathsf{R}}\mathsf{R}(\mathsf{R}-1)\frac{\partial}{\partial \mathsf{R}}{}^{(k)}F_2^{(V)\mathrm{Sch}} = {}^{(k)}\mathcal{S}_2^{(V)}, \tag{3.32}$$

$$\frac{\partial}{\partial \mathsf{R}}\mathsf{R}(\mathsf{R}-1)\frac{\partial}{\partial \mathsf{R}}{}^{(k)}F_3^{(V)\mathrm{Sch}} = {}^{(k)}\mathcal{S}_3^{(V)}. \tag{3.33}$$

The leading order solution satisfying the regularity condition on the horizon and at infinity is given by

$${}^{(0)}F_{00}^{(S)\mathrm{Sch}} = \frac{A(\theta)}{\mathsf{R}-1}, \qquad {}^{(0)}F_{01}^{(S)\mathrm{Sch}} = \frac{A(\theta)}{\mathsf{R}-1}, \ {}^{(0)}F_{02}^{(S)\mathrm{Sch}} = \frac{B(\theta)}{\sqrt{\mathsf{R}(\mathsf{R}-1)}}, \tag{3.34}$$

$${}^{(0)}F_{03}^{(S)\mathrm{Sch}} = \frac{C(\theta)}{\sqrt{\mathsf{R}(\mathsf{R}-1)}}, \ {}^{(0)}F_{11}^{(S)\mathrm{Sch}} = \frac{D(\theta)}{\mathsf{R}}, \ {}^{(0)}F_{12}^{(S)\mathrm{Sch}} = \frac{B(\theta)}{\sqrt{\mathsf{R}(\mathsf{R}-1)}}, \tag{3.35}$$

$${}^{(0)}F_{13}^{(S)\mathrm{Sch}} = \frac{C(\theta)}{\sqrt{\mathsf{R}(\mathsf{R}-1)}}, \ {}^{(0)}F_{22}^{(S)\mathrm{Sch}} = 0, \qquad {}^{(0)}F_{23}^{(S)\mathrm{Sch}} = 0, \qquad {}^{(0)}F_{33}^{(S)\mathrm{Sch}} = 0, \tag{3.36}$$

for the scalar type perturbation and

$${}^{(0)}F_0^{(V)\mathrm{Sch}} = \frac{W(\theta)}{\sqrt{\mathsf{R}(\mathsf{R}-1)}}, \ {}^{(0)}F_1^{(V)\mathrm{Sch}} = \frac{W(\theta)}{\sqrt{\mathsf{R}(\mathsf{R}-1)}}, \ {}^{(0)}F_2^{(V)\mathrm{Sch}} = {}^{(0)}F_3^{(V)\mathrm{Sch}} = 0, \tag{3.37}$$

for the vector type perturbation. The leading order perturbation solution contains undetermined integration functions $A(\theta)$, $B(\theta)$, $C(\theta)$, $D(\theta)$ and $W(\theta)$ for each type perturbation. If we go to the higher order of k we can obtain the non-trivial relation between integration functions. Especially the solution at $k = 1$ and $k = 2$ order gives quasinormal mode frequency of the Schwarzschild black hole for the vector and scalar type perturbation respectively. The detail analysis and results of this will be given in section 4 and appendix D.

3.2 Stationary solution

We apply the boost transformation to the perturbation solution of the Schwarzschild black hole. At first, before taking large D limit, we give the general procedure for the perturbation of the stationary black hole solution given by

$$\begin{aligned} ds^2 = &-A(\rho,z)^2dt^2 + B(\rho.z)^2d\rho^2 + F(\rho,z)^2(d\phi - w(\rho,z)dt)^2 \\ &+ G(\rho,z)^2dz^2 + H(\rho,z)^2d\Omega_{D-4}^2. \end{aligned} \tag{3.38}$$

We consider the scalar and vector type perturbation on S^{D-4}. To give perturbation variables we use the following vielbein

$$e^{(0)} = A(\rho,z)dt, \qquad e^{(1)} = B(\rho,z)d\rho, \qquad e^{(2)} = F(\rho,z)(d\phi - w(\rho,z)dt) \tag{3.39}$$

JHEP09(2015)193

and

$$e^{(3)} = G(\rho, z)dz, \qquad e^{(A)} = H(\rho, z)\hat{e}^{(A)}, \tag{3.40}$$

where $\hat{e}^{(A)}$ is the vielbein on the unit sphere S^{D-4} again. Then the perturbed metric $h_{\mu\nu}$ is given by the components with respect to these vielbeins as

$$h^{(S)}_{\mu\nu}dx^\mu dx^\nu = e^{-i\omega t}e^{im\phi}\Big[f^{(S)}_{IJ}\mathbb{Y}^{(S)}_j e^{(I)}e^{(J)} + f^{(S)}_I \mathsf{D}_A \mathbb{Y}^{(S)}_j e^{(I)}e^{(A)} \\ + H(\rho,z)^2(H^{(S)}_T \mathbb{Y}^{(S)}_j q_{AB} + H^{(S)}_L \mathbb{Y}^{(S)j}_{AB})dx^A dx^B\Big], \tag{3.41}$$

for scalar type perturbation and

$$h^{(V)}_{\mu\nu}dx^\mu dx^\nu = e^{-i\omega t}e^{im\phi}\Big[f^{(V)}_I \mathbb{Y}^{(V)j}_A e^{(I)}e^{(A)} + H^{(V)}_L \mathbb{Y}^{(V)j}_{AB} e^{(A)}e^{(B)}\Big], \tag{3.42}$$

for the vector type perturbation. Then we perform the boost transformation on these perturbed metrics of the leading order solution obtained in section 2. The boost transformation gives the relation between vielbeins as

$$e^{(0)}_{\rm Sch} \to \frac{2 - r_0(z)^2(1-\sinh^2\rho)}{r_0(z)^2\cosh\rho\sqrt{1+r_0(z)^2\sinh^2\rho}}e^{(0)} - \sinh\rho\sqrt{\frac{1-r_0(z)^2}{1+r_0(z)^2\sinh^2\rho}}e^{(2)}, \tag{3.43}$$

$$e^{(2)}_{\rm Sch} \to \frac{\cosh\rho}{\sqrt{1+r_0(z)^2\sinh^2\rho}}e^{(2)} - \frac{2+r_0(z)^2\sinh^2\rho}{r_0\sinh\rho}\sqrt{\frac{1-r_0(z)^2}{1+r_0(z)\sinh^2\rho}}e^{(0)}, \tag{3.44}$$

where we used the vielbein of the Schwarzschild black hole (3.7) and of the stationary solution (3.39) for the leading order metric (2.61).[7] This relation between vielbeins gives also the relation between the perturbation variables of the Schwarzschild black hole and general stationary solutions. Since we know the decoupled perturbation variables on the Schwarzschild black hole, we can obtain the following decoupled perturbation variables, $F^{(S)}_{IJ}$, $F^{(S)}_I$, $F^{(S)}_{T,L}$, $F^{(V)}_I$ and $F^{(V)}_L$ of the general stationary solution at large D as

$$F^{(S)}_{00} = \frac{\cosh^2\rho}{1+r_0(z)^2\sinh^2\rho}f^{(S)}_{00} - \frac{2\sinh\rho\cosh\rho\sqrt{1-r_0(z)^2}}{1+r_0(z)^2\sinh^2\rho}f^{(S)}_{02} \\ + \frac{(1-r_0(z)^2)\sinh^2\rho}{1+r_0(z)^2\sinh^2\rho}f^{(S)}_{22} + f^{(S)}_{11}, \tag{3.45}$$

$$F^{(S)}_{11} = \frac{\cosh^2\rho}{1+r_0(z)^2\sinh^2\rho}f^{(S)}_{00} - \frac{2\sinh\rho\cosh\rho\sqrt{1-r_0(z)^2}}{1+r_0(z)^2\sinh^2\rho}f^{(S)}_{02} \\ + \frac{(1-r_0(z)^2)\sinh^2\rho}{1+r_0(z)^2\sinh^2\rho}f^{(S)}_{22} - f^{(S)}_{11}, \tag{3.46}$$

$$F^{(S)}_{02} = \frac{\cosh^2\rho - (1-r_0(z)^2)\sinh^2\rho}{1+r_0(z)^2\sinh^2\rho}f^{(S)}_{02} \\ - \frac{\sqrt{1-r_0(z)^2}\sinh\rho\cosh\rho}{1+r_0(z)^2\sinh^2\rho}(f^{(S)}_{00} + f^{(S)}_{02}), \tag{3.47}$$

[7] We consider the asymptotically flat black hole $\mathsf{V}_0(z) = 1$.

JHEP09(2015)193

$$F_{22}^{(S)} = \frac{\cosh^2\rho}{1+r_0(z)^2\sinh^2\rho} f_{22}^{(S)} - \frac{2\sinh\rho\cosh\rho\sqrt{1-r_0(z)^2}}{1+r_0(z)^2\sinh^2\rho} f_{02}^{(S)} + \frac{(1-r_0(z)^2)\sinh^2\rho}{1+r_0(z)^2\sinh^2\rho} f_{00}^{(S)}, \tag{3.48}$$

$$F_{01}^{(S)} = \frac{\cosh\rho}{\sqrt{1+r_0(z)^2\sinh^2\rho}} f_{01}^{(S)} - \sinh\rho\sqrt{\frac{1-r_0(z)^2}{1+r_0(z)^2\sinh^2\rho}} f_{12}^{(S)}, \tag{3.49}$$

$$F_{12}^{(S)} = \frac{\cosh\rho}{\sqrt{1+r_0(z)^2\sinh^2\rho}} f_{12}^{(S)} - \sinh\rho\sqrt{\frac{1-r_0(z)^2}{1+r_0(z)^2\sinh^2\rho}} f_{01}^{(S)}, \tag{3.50}$$

$$F_{03}^{(S)} = \frac{\cosh\rho}{\sqrt{1+r_0(z)^2\sinh^2\rho}} f_{03}^{(S)} - \sinh\rho\sqrt{\frac{1-r_0(z)^2}{1+r_0(z)^2\sinh^2\rho}} f_{23}^{(S)}, \tag{3.51}$$

$$F_{23}^{(S)} = \frac{\cosh\rho}{\sqrt{1+r_0(z)^2\sinh^2\rho}} f_{23}^{(S)} - \sinh\rho\sqrt{\frac{1-r_0(z)^2}{1+r_0(z)^2\sinh^2\rho}} f_{03}^{(S)}, \tag{3.52}$$

$$F_{0}^{(S)} = \frac{\cosh\rho}{\sqrt{1+r_0(z)^2\sinh^2\rho}} f_{0}^{(S)} - \sinh\rho\sqrt{\frac{1-r_0(z)^2}{1+r_0(z)^2\sinh^2\rho}} f_{2}^{(S)}, \tag{3.53}$$

$$F_{2}^{(S)} = \frac{\cosh\rho}{\sqrt{1+r_0(z)^2\sinh^2\rho}} f_{2}^{(S)} - \sinh\rho\sqrt{\frac{1-r_0(z)^2}{1+r_0(z)^2\sinh^2\rho}} f_{0}^{(S)}, \tag{3.54}$$

and

$$F_{13}^{(S)} = f_{13}^{(S)}, \qquad F_{33}^{(S)} = f_{33}^{(S)}, \qquad F_{1}^{(S)} = f_{1}^{(S)}, \qquad F_{3}^{(S)} = f_{3}^{(S)}, \qquad F_{T,L}^{(S)} = H_{T,L}^{(S)}, \tag{3.55}$$

for the scalar type perturbation and

$$F_{0}^{(V)} = \frac{\cosh\rho}{\sqrt{1+r_0(z)^2\sinh^2\rho}} f_{0}^{(V)} - \sinh\rho\sqrt{\frac{1-r_0(z)^2}{1+r_0(z)^2\sinh^2\rho}} f_{2}^{(V)}, \tag{3.56}$$

$$F_{2}^{(V)} = \frac{\cosh\rho}{\sqrt{1+r_0(z)^2\sinh^2\rho}} f_{2}^{(V)} - \sinh\rho\sqrt{\frac{1-r_0(z)^2}{1+r_0(z)^2\sinh^2\rho}} f_{0}^{(V)}, \tag{3.57}$$

and

$$F_{1}^{(V)} = f_{1}^{(V)}, \qquad F_{3}^{(V)} = f_{3}^{(V)}, \qquad F_{L}^{(V)} = H_{L}^{(V)}, \tag{3.58}$$

for the vector type perturbation. Each perturbation variables are expanded at large D as

$$F_{IJ}^{(S)} = \sum_{k\geq 0} \frac{{}^{(k)}F_{IJ}^{(S)}}{n^k}, \; F_{I}^{(S)} = \sum_{k\geq 0} \frac{{}^{(k)}F_{I}^{(S)}}{n^k}, \; F_{T,L}^{(S)} = \sum_{k\geq 0} \frac{{}^{(k)}F_{T,L}^{(S)}}{n^k}, \tag{3.59}$$

and

$$F_{I}^{(V)} = \sum_{k\geq 0} \frac{{}^{(k)}F_{I}^{(V)}}{n^k}, \; F_{T,L}^{(V)} = \sum_{k\geq 0} \frac{{}^{(k)}F_{L}^{(V)}}{n^k}. \tag{3.60}$$

JHEP09(2015)193

Then the perturbation equation for these decoupling variables can be obtained from the Lichnerowicz equation under the transverse traceless gauge condition. Now we have obtained the leading order metric of the stationary black hole in the $1/D$ expansion in section 2. Then the perturbation equation for $k = 0$ order is also obtained by using the leading order metric. The perturbation equation of the decoupling variables can be found to satisfy same equations with one of the Schwarzschild black hole at the leading order by changing the radial coordinate from ρ to R by[8]

$$\mathsf{R} = \cosh^2 \rho. \tag{3.61}$$

At higher orders the perturbation equation of the stationary solution becomes different from the boosted one of the Schwarzschild black hole in source terms. This is because the boost relation is valid only in the leading order metric, and higher order structure gives the essential effect coming from the difference from the Schwarzschild black holes. However the homogeneous part of the equation at each order is always same with one of the Schwarzschild black hole. So, in principle, the perturbation equation is a set of decoupled ordinarily differential equations and we can solve it by a straightforward integration method with the Green's function.

The regular leading order solution of the perturbation equation for the stationary black hole is

$$ {}^{(0)}F_{00}^{(S)} = \frac{A(\theta)}{\mathsf{R}-1}, \qquad {}^{(0)}F_{01}^{(S)} = \frac{A(\theta)}{\mathsf{R}-1}, \qquad {}^{(0)}F_{02}^{(S)} = \frac{B(\theta)}{\sqrt{\mathsf{R}(\mathsf{R}-1)}}, \tag{3.62}$$

$$ {}^{(0)}F_{03}^{(S)} = \frac{C(\theta)}{\sqrt{\mathsf{R}(\mathsf{R}-1)}}, \qquad {}^{(0)}F_{11}^{(S)} = \frac{D(\theta)}{\mathsf{R}}, \qquad {}^{(0)}F_{12}^{(S)} = \frac{B(\theta)}{\sqrt{\mathsf{R}(\mathsf{R}-1)}}, \tag{3.63}$$

$$ {}^{(0)}F_{13}^{(S)} = \frac{C(\theta)}{\sqrt{\mathsf{R}(\mathsf{R}-1)}}, \qquad {}^{(0)}F_{22}^{(S)} = 0, \qquad {}^{(0)}F_{23}^{(S)} = 0, \qquad {}^{(0)}F_{33}^{(S)} = 0, \tag{3.64}$$

for the scalar type perturbation and

$$ {}^{(0)}F_{0}^{(V)} = \frac{W(\theta)}{\mathsf{R}}, \qquad {}^{(0)}F_{1}^{(V)} = \frac{W(\theta)}{\mathsf{R}}, \qquad {}^{(0)}F_{2}^{(V)} = {}^{(0)}F_{3}^{(V)} = 0, \tag{3.65}$$

for the vector type perturbation. In the derivation of the perturbation equations and solutions we need only the leading order solution of general stationary solutions given in section 2. To go to more higher order perturbation equations, the higher order solutions of stationary solutions are required. In the next section we consider the higher order perturbation equation of the Myers-Perry black hole, which is a known exact solution.

Note that the quasinormal mode frequency of the decoupled mode perturbation is obtained by solving higher order perturbation equation in $1/D$. The higher order structure of the perturbation equation reflects the higher order structure of the background metric, which does not have the boost property. Hence the frequency does not have the boost property either. This implies that the quasinormal mode frequency of the Myers-Perry black

[8]This relation can be understood by the horizon position. The Schwarzschild black hole has the horizon at $\mathsf{R} = 1$ and the general stationary black hole horizon position is set to be $\rho = 0$.

JHEP09(2015)193

hole cannot be obtained by the boost transformation from one of the Schwarzschild black hole. This non-boost property allows the existence of the instability mode in the decoupled sector of the perturbation of the Myers-Perry black hole. In contrast the quasinormal mode of the non-decoupled sector perturbation is obtained in the leading order structure and we expect that such mode has the boost property as the universal feature [5].

4 QNMs of Myers-Perry black hole

We pursue the decoupling property of perturbation variables at large D expansion shown in the previous section to more higher order structure to obtain the quasinormal mode (QNM) frequency of the $D = n + 3$ dimensional singly rotating Myers-Perry black hole. This was calculated numerically in [29] for non-axisymmetric perturbations. Here we give the analytic formula of the QNM frequency both for the axisymmetric and non-axisymmetric perturbations. The metric of the Myers-Perry black hole is given in the appendix A and it is written by the following parameter setting

$$\mathsf{V}_0(z) = 1, \qquad \hat{\kappa} = \frac{1}{2}, \qquad \Omega_H = \frac{a}{1+a^2}, \qquad R(\theta) = \cos\theta, \qquad r_0(\theta)^{-2} = \frac{1+a^2}{1+a^2\cos^2\theta}, \tag{4.1}$$

in the leading order metric obtained in section 2. Our detail analysis in this section concentrates on the scalar type perturbation since the analysis of the vector type perturbation is performed in the same manner. The only result of the QNM frequency for the vector type perturbation will be given later. The scalar type perturbation variables are defined in the same way with one in section 3 as

$$h_{\mu\nu}dx^\mu dx^\nu = e^{-i\omega t}e^{im\phi}\Big[f_{ab}\mathbb{Y}^{(S)}_j e^{(a)}e^{(b)} + f_a \mathsf{D}_A\mathbb{Y}^{(S)}_j e^{(a)}e^{(A)} + r^2\cos^2\theta(H_T\mathbb{Y}^{(S)}_j q_{AB} + H_L\mathbb{Y}^{(S)j}_{AB})dx^A dx^B\Big], \tag{4.2}$$

where the vielbein was defined in section 3.[9] So the perturbation is parameterized by ω, m and j. j describes the deformation parameter on S^{D-4}. Thus $j = 0$ correspond to the perturbation without the deformation on S^{D-4}. Then the decoupled perturbation variables can be constructed and expanded at large D as

$$F_{IJ} = \sum_{k\geq 0}\frac{F^{(k)}_{IJ}}{n^k}, \qquad F_a = \sum_{k\geq 0}\frac{F^{(k)}_a}{n^k}, \qquad F_{T,L} = \sum_{k\geq 0}\frac{F^{(k)}_{T,L}}{n^k}, \tag{4.3}$$

where $D = n + 3$. The boundary condition for the perturbation on the horizon is the ingoing boundary condition [29] as

$$h_{\mu\nu}(r,\theta) = \hat{h}_{\mu\nu}(r,\theta)(r-r_+)^{-i(\omega-m\Omega_H)/2\kappa}, \tag{4.4}$$

where r_+ is the horizon position and κ is a surface gravity. The component of $\hat{h}_{\mu\nu}$ in the Eddington-Finkelstein ingoing coordinate should be regular on the horizon. Here we omit

[9] We omit the index $^{(S)}$ representing the scalar type perturbation in section 3.

JHEP09(2015)193

the t, ϕ and x^A dependence just for the simplicity.[10] The boundary condition at infinity $\mathsf{R} \gg 1$ is the decoupled mode condition [7] as

$$h_{\mu\nu} = O(\mathsf{R}^{-1}). \tag{4.5}$$

This condition is equivalent to the outgoing wave boundary condition at infinity for the decoupled mode defined by $\omega r_0 = O(D^0)$.

In the following we give the brief summary of perturbation solutions of the scalar type perturbation up to $k = 2$ order. At $k = 2$ we obtain QNM frequency for the first time.

Leading order solution ($k = 0$). The leading order solution satisfying the boundary conditions is

$$\begin{aligned}
&F^{(0)}_{00} = \frac{A_{(0)}(\theta)}{\mathsf{R}-1}, && F^{(0)}_{01} = \frac{A_{(0)}(\theta)}{\mathsf{R}-1}, && F^{(0)}_{02} = \frac{B_{(0)}(\theta)}{\sqrt{\mathsf{R}(\mathsf{R}-1)}},\\
&F^{(0)}_{03} = \frac{C_{(0)}(\theta)}{\sqrt{\mathsf{R}(\mathsf{R}-1)}}, && F^{(0)}_{11} = \frac{D_{(0)}(\theta)}{\mathsf{R}}, && F^{(0)}_{12} = \frac{B_{(0)}(\theta)}{\sqrt{\mathsf{R}(\mathsf{R}-1)}},\\
&F^{(0)}_{13} = \frac{C_{(0)}(\theta)}{\sqrt{\mathsf{R}(\mathsf{R}-1)}}, && F^{(0)}_{22} = 0, && F^{(0)}_{23} = 0, \qquad F^{(0)}_{33} = 0.
\end{aligned} \tag{4.6}$$

At leading order we have four independent integration functions, which cannot be determined by the boundary condition. The solution for $F^{(0)}_I$ and $F^{(0)}_{T,L}$ can be obtained by the transverse traceless gauge condition, and we omit them since it is not so important.

Next to leading order solution ($k = 1$). The next to leading order solution of F_{IJ} is represented by

$$\begin{aligned}
&F^{(1)}_{00} = \frac{A_{(1)}(\theta)}{\mathsf{R}-1} + \hat{F}^{(1)}_{00}, && F^{(1)}_{01} = \frac{A_{(1)}(\theta)}{\mathsf{R}-1} + \hat{F}^{(1)}_{01},\\
&F^{(1)}_{02} = \frac{B_{(1)}(\theta)}{\sqrt{\mathsf{R}(\mathsf{R}-1)}} + \hat{F}^{(1)}_{02}, && F^{(1)}_{03} = \frac{C_{(1)}(\theta)}{\sqrt{\mathsf{R}(\mathsf{R}-1)}} + \hat{F}^{(1)}_{03},\\
&F^{(1)}_{11} = \frac{D_{(1)}(\theta)}{\mathsf{R}} + \hat{F}^{(1)}_{11}, && F^{(1)}_{12} = \frac{B_{(1)}(\theta)}{\sqrt{\mathsf{R}(\mathsf{R}-1)}} + \hat{F}^{(1)}_{12},\\
&F^{(1)}_{13} = \frac{C_{(1)}(\theta)}{\sqrt{\mathsf{R}(\mathsf{R}-1)}} + \hat{F}^{(1)}_{13}, && F^{(1)}_{22} = \hat{F}^{(1)}_{22}, \quad F^{(1)}_{23} = 0, \quad F^{(1)}_{33} = \hat{F}^{(1)}_{33},
\end{aligned} \tag{4.7}$$

where the solution with the hat comes from the integration of the source term composed by the leading order solution. At this order we have new four integration functions $A_{(1)}(\theta)$, $B_{(1)}(\theta)$, $C_{(1)}(\theta)$ and $D_{(1)}(\theta)$. To satisfy boundary conditions we obtain some non-trivial relations for $A_{(0)}(\theta)$, $B_{(0)}(\theta)$, $C_{(0)}(\theta)$ and $D_{(0)}(\theta)$. Conditions we find are

$$B_{(0)}(\theta) = 0, \qquad C_{(0)}(\theta) = 0, \tag{4.8}$$

[10] x^A is a coordinate on S^{D-4}.

JHEP09(2015)193

and

$$\cos\theta(1+a^2\cos^2\theta)\left((1+a^2)\cos\theta A_{(0)}(\theta)-\sin\theta D'_{(0)}(\theta)\right)$$
$$+\left[j+(-1+iam+a^2(-3+2j-i\omega)-i\omega)\cos^2\theta\right.$$
$$\left.+a^2(1+iam+a^2(j-1-i\omega)-i\omega)\cos^4\theta\right]D_{(0)}(\theta)=0. \tag{4.9}$$

Using this condition we can eliminate $A_{(0)}(\theta)$. To obtain QNM frequency we should specify the function $D_{(0)}(\theta)$, and we can do it at next to next to leading order.

Next-to-next-to leading order solution ($k=2$). At this order we can obtain the solutions in the same way with the next to leading order. We find additional non-trivial condition for integration functions. By eliminating $A_{(0)}(\theta)$, the additional conditions are written as

$$c_1(\theta)C''_{(1)}(\theta)+c_2(\theta)C'_{(1)}(\theta)+c_3(\theta)C_{(1)}(\theta)$$
$$+c_4(\theta)D''_{(0)}(\theta)+c_5(\theta)D'_{(0)}(\theta)+c_6(\theta)D_{(0)}(\theta)=0, \tag{4.10}$$

and

$$d_1(\theta)D'''_{(0)}(\theta)+d_2(\theta)D''_{(0)}(\theta)+d_3(\theta)D'_{(0)}(\theta)$$
$$+d_4(\theta)D_{(0)}(\theta)+d_5(\theta)C'_{(1)}(\theta)+d_6(\theta)C_{(1)}(\theta)=0. \tag{4.11}$$

Each functions $c_i(\theta)$ and $d_i(\theta)$ have messy forms so we do not show them here. They are given in the appendix E. In general it seems that we should solve these differential equations to obtain the QNM frequency. However, we find that the QNM frequency can be obtained only from the boundary conditions.[11] At $\theta=\pi/2$ the boundary condition is read from eqs. (4.10) and (4.11) as

$$C_{(1)}(\theta)|_{\theta=\pi/2}=\cos^{j-3}\theta, \qquad D_{(0)}(\theta)|_{\theta=\pi/2}=\cos^{j}\theta. \tag{4.12}$$

On the other hand the behavior at $\theta=0$ is

$$C_{(1)}(\theta)|_{\theta=0}=\sin^{\delta^S_\omega-1}\theta, \qquad D_{(0)}(\theta)|_{\theta=0}=\sin^{\delta^S_\omega}\theta, \tag{4.13}$$

where δ^S_ω depends on a, m, j and ω. To see which value δ^S_ω should take, we observe the spherical harmonics, $\mathbb{S}^\ell(\theta)e^{im\phi}\mathbb{Y}^{(S)}_j$, on S^{D-2}, defined by

$$\left[\Delta_{S^{D-2}}+\ell(\ell+D-3)\right]\mathbb{S}^\ell e^{im\phi}\mathbb{Y}^{(S)}_j$$
$$=\left[\frac{1}{\sin\theta\cos^{D-4}\theta}\frac{d}{d\theta}\left(\sin\theta\cos^{D-4}\theta\frac{d}{d\theta}\mathbb{S}^\ell\right)\right.$$
$$\left.-\frac{m^2}{\sin^2\theta}\mathbb{S}^\ell-\frac{j(j+D-5)}{\cos^2\theta}\mathbb{S}^\ell+\ell(\ell+D-3)\mathbb{S}^\ell\right]e^{im\phi}\mathbb{Y}^{(S)}_j=0. \tag{4.14}$$

[11] Actually we can confirm that eqs. (4.10) and (4.11) can be solved regularly under the QNM frequency obtained below. Thus there may be some non-trivial structure in the solutions of eqs. (4.10) and (4.11) and the boundary conditions.

JHEP09(2015)193

The solution of this equation can be written by the hypergeometric function as

$$\mathbb{S}^\ell = \cos^j\theta \ \sin^{|m|}\theta \ {}_2F_1(-k_S, k_S + |m| + j + n/2, |m| + 1; \sin^2\theta), \tag{4.15}$$

where k_S is a non-negative integer satisfying

$$\ell = j + |m| + 2k_S. \tag{4.16}$$

At large D this solution becomes

$$\begin{aligned}\mathbb{S}^\ell &= \sin^{\ell-j}\theta\cos^j\theta + O(1/D) \\ &= \sin^{|m|+2k_S}\theta\cos^j\theta + O(1/D).\end{aligned} \tag{4.17}$$

k_S describes the overtone number of $\mathbb{S}^\ell$ along θ direction, and this overtone number can be observed from the behavior of $\mathbb{S}^\ell$ at $\theta = 0$ at large D limit as seen eq. (4.17). From this observation on the spherical harmonics we impose the following condition on δ^S_ω as the harmonics condition

$$\begin{aligned}\delta^S_\omega &= \ell - j \\ &= 2k_s + |m|,\end{aligned} \tag{4.18}$$

where ℓ is parametrized as eq. (4.16) by non-negative integer k_S. Then eqs. (4.10) and (4.11) under the condition (4.18) give one non-trivial algebraic condition on ω. This non-trivial condition on ω can be regarded as the QNM condition. In the following we solve the condition eq. (4.18) for ω in some cases. The explicit form of the QNM condition (4.18) is given in the appendix F.

Note that the condition (4.18) is equivalent to the regularity condition to derive eq. (2.56) in section 2. The condition (4.18) is suggested by the analysis for spherical harmonics at large D. However, as we can see in appendix C, the analysis of the spheroidal harmonics also gives same condition (4.18). Thus we expect that the condition (4.18) would hold also in the gravitational perturbation of the Myers-Perry black hole.

4.1 QNM frequency

We show some explicit results of the QNM frequency of the scalar and vector type perturbations by solving the QNM condition (4.18). The instability exists only in the scalar type perturbation and the vector type perturbation is always stable for the decoupled sector perturbation.[12] We set the horizon radius to unity as

$$r_0 = 1, \tag{4.19}$$

by fixing the unit.

[12]The instability mode is conjectured to exist only in the decoupled sector (saturated mode) [29]. The tensor type perturbation of the singly rotating Myers-Perry black hole does not have the decoupled sector and it was shown to be stable [31].

JHEP09(2015)193

4.1.1 Scalar type perturbation

The QNM frequency is given by the solution of the algebraic equation (4.18), which can be solved analytically. We solve eq. (4.18) for some cases below. Since the $j \neq 0$ modes do not show any instability, we consider only $j = 0$ modes. The perturbation with $j \neq 0$ describes the deformation of S^{D-4} of the Myers-Perry black hole. So we might be able to say that the axisymmetric instability occurs only in the "S-wave" sector in the perturbation similar to the Gregory-Laflamme instability of the black brane [32, 33].

Then, for this mode, the quasinormal mode condition (4.18) can be written in a relatively simple form as

$$\begin{aligned}
&(1+a^2)^3\omega^3 - (1+a^2)^2(4i - 3\ell + 3am)\omega^2 \\
&\quad + (1+a^2)(-4 + 7\ell - 3\ell^2 - 6iam(\ell-1) + a^2 - 4 + 3\ell + 3m^2)\omega \\
&\quad + (-i\ell^3 + \ell^2(3i + ia^2 + 3am) - \ell(2i + 5am + a^3 m - ia^2(-2+3m^2)) \\
&\qquad + am(2 - 2iam - a^2(m^2 - 2))) = 0.
\end{aligned} \tag{4.20}$$

At $a = 0$ the scalar type perturbation has the physical degree of freedom for $\ell \geq 2$ [30] and, hence, we study the modes of $\ell \geq 2$.

Schwarzschild black hole. At $a = 0$ where the solution is the Schwarzschild black hole we can solve eq. (4.20) explicitly by

$$\omega = \pm\sqrt{\ell - 1} - i(\ell - 1), \qquad \omega = -i\ell. \tag{4.21}$$

These modes correspond to the decoupled scalar and vector type mode of Schwarzschild black hole on S^{D-2} [7].

Axisymmetric perturbation. Next we consider the axisymmetric perturbation $m = 0$ with $a \neq 0$. In this perturbation we find that there are stationary perturbations $\omega = 0$ at a_c where

$$\begin{aligned}
a_c^2 &= \ell - 1 \\
&= 2k_S - 1,
\end{aligned} \tag{4.22}$$

and we used eq. (4.16) with $j = m = 0$. The assumption of $\ell \geq 2$ implies $k_S \geq 1$ for $j = m = 0$, and this result reproduces the result (2.56) derived from the effective theory obtained in section 2. In figure 1 we give the plot of the QNM frequency with $(\ell, m, j) = (4, 0, 0)$. The black thick line, purely imaginary frequency mode, shows the instability mode and it becomes the marginally stable mode at $a_c^2 = 3$. For the axisymmetric perturbation with $\omega = 0$ and $j = 0$ we can solve eqs. (4.10) and (4.11) explicitly by

$$C_0(\theta) = 0, \qquad D_0(\theta) = \tilde{D}_0 \frac{\sin^{1+a^2}\theta}{1 + a^2\cos^2\theta}, \tag{4.23}$$

where $\tilde{D}_0$ is a constant. Then we can see that this stationary solution is equivalent to the perturbation solution (2.55) obtained in the effective theory. This equivalence suggests the validity of our QNM condition (4.18).

JHEP09(2015)193

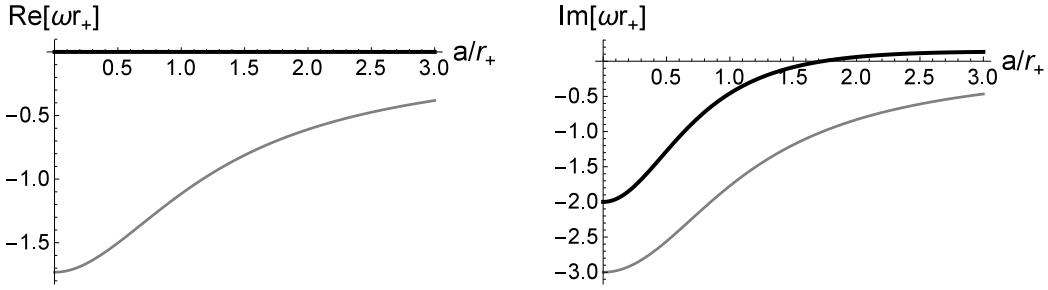

Figure 1. The QNM frequency for $(\ell, m, j) = (4, 0, 0)$. The black thick line is the pure imaginary mode and it shows the instability at $a^2 > 3$. The gray thick line is the stable mode.

Non-axisymmetric perturbation. The non-axisymmetric mode perturbation also shows the instability at $a^2 > a_c^2$ where a_c is given in eq. (4.22) as

$$\begin{aligned} a_c^2 &= \ell - 1 \\ &= |m| + 2k_S - 1. \end{aligned} \tag{4.24}$$

At the critical rotation the instability mode satisfies the superradiance condition as

$$\omega|_{a=a_c} = \frac{a_c m}{1 + a_c^2} = m\Omega_H(a_c). \tag{4.25}$$

Hence the dynamical instability mode shows the superradiance instability at the same time. This coincidence of the onsets of dynamical and superradiant instability has been also observed in the QNMs of the Myers-Perry black hole with equal spin [6] up to $O(1/D)$ correction. The numerical results [34] also suggest the coincidence for the equal spin case. On the other hand the numerical analysis of QNMs of the singly rotating Myers-Perry black hole does not show such coincidence [29, 35]: the superradiant instability appears at slower rotation than the critical rotation of the dynamical instability. Thus our coincidence is just the property only at large D limit. If one considers $1/D$ corrections of QNMs of singly rotating Myers-Perry black hole, there would be a difference between the onset of the superradiant and dynamical instability.

For the bar mode defined by $m = \ell$, we can solve eq. (4.20) explicitly by

$$\omega_\pm = \frac{\pm\sqrt{m-1} + a(m-1)}{1+a^2} - i\frac{m - 1 \mp a\sqrt{m-1}}{1+a^2}, \qquad \omega_{(0)} = \frac{am}{1+a^2} - i\frac{m}{1+a^2}. \tag{4.26}$$

ω_+ shows the instability at $a > a_c$ and saturates the superradiance condition at $a = a_c$. In figure 2 we show the plot of the bar mode QNM frequency for $m = 2$. The QNM frequency for the bar mode was obtained numerically in [29]. The behavior of the frequency shows good agreements with our analytic results.

The non-axisymmetric perturbation with $\ell > m$ also shows the instability. But its origin is different from one of the bar mode. The instability mode of the bar mode perturbation comes from the scalar type perturbation of the Schwarzschild black hole at $a = 0$ where the frequency is complex (see eq. (4.21)). On the other hand non-axisymmetric mode with $\ell > m$ has an instability in the mode coming from the vector type perturbation

JHEP09(2015)193

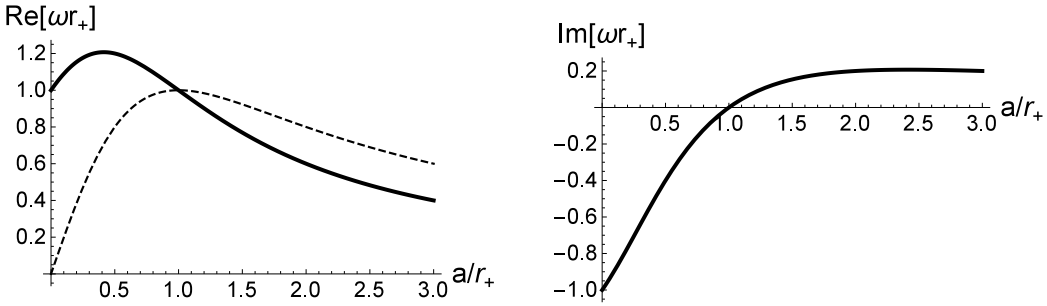

Figure 2. The plot of the bar mode QNM frequency of $(\ell, m, j) = (2, 2, 0)$ is shown. The black dashed line is the superradiance condition. The onset of the dynamically unstable mode is same as the one of the superradiance instability.

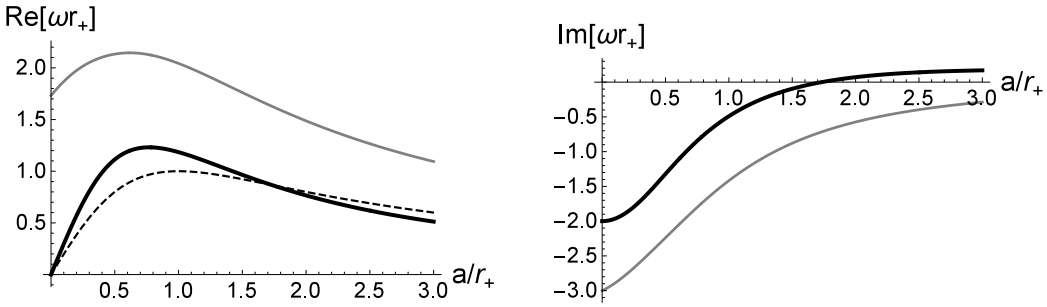

Figure 3. The plot of the QNM frequency of $(\ell, m, j) = (4, 2, 0)$ is shown. The black dashed line is the superradiance condition. The gray thick line is the stable mode ω_-, while the black thick line shows the unstable mode ω_+. The dynamical instability appears exactly when the superradiance condition is satisfied.

of the Schwarzschild black hole, whose frequency is a pure imaginary as (4.21). This is same situation with the perturbation of the Myers-Perry black hole with equal spin [6]. In figure 3 we give the plot of QNM frequency for $\ell = 4$, $m = 2$. As we can see, the mode showing instability becomes purely imaginary at $a = 0$, which corresponds to the vector type perturbation of the Schwarzschild black hole.

4.1.2 Vector type perturbation

The QNM frequency of the vector type perturbation can be given as

$$\omega^V = \omega^V_{\rm LO} + \frac{\omega^V_{\rm NLO}}{n} + O(1/n^2), \tag{4.27}$$

where

$$\omega^V_{\rm LO} = \frac{am}{1+a^2} - i\left(j - 1 + \frac{\ell - j}{1+a^2}\right), \tag{4.28}$$

JHEP09(2015)193

and

$$\omega^V_{\rm NLO} = \frac{2am}{1+a^2}\Big(\ell - 1 + a^2(j-1) + \log(1+a^2)\Big) - i\Bigg((j-1)^2 + \frac{(1+a^2)(\ell-j)(\ell+j-2) - 2a^2m^2}{(1+a^2)^2} + \left(j - 1 - \frac{\ell-j}{1+a^2} + \frac{2(\ell-j)}{(1+a^2)^2}\right)\log(1+a^2)\Bigg). \tag{4.29}$$

We have solved the perturbation equation up to $k = 2$ order and obtained the QNM frequency up to $1/D$ correction. This QNM frequency is obtained by imposing the same harmonics condition with the scalar type perturbation on the behavior at $\theta = 0$ motivated by eq. (4.17). The QNM frequency (4.28) reduces to the vector type perturbation on S^{D-2} of the Schwarzschild black hole [7] at $a = 0$ as

$$\omega = -i(\ell-1)\left(1 + \frac{\ell-1}{n} + O(1/n^2)\right). \tag{4.30}$$

5 Summary

The large D expansion method has been found to be useful to solve the gravitational problem as shown in [1–10]. In this paper we have performed the next step for the further developing of the large D expansion method by constructing the effective theory of the large D stationary black hole in asymptotically flat or AdS spacetime. Considering the additional degree of freedom of the horizon, *rotation radius of the black hole*, the effective theory becomes non-trivial and allows the existence of various solutions compared to the static case in the asymptotically flat spacetime which has only one unique solution, Schwarzschild black hole [9]. This new degree of freedom appears as the Lorentz boost of the black hole along the rotational direction, and we can rewrite the solution of the effective equation in very simple and illuminative expression by using this boost property.

As applications of the effective theory we have considered the ellipsoidal embeddings and obtained the Myers-Perry black hole and bumpy black hole solutions in perturbative manner. Then we have succeeded to derive the threshold angular momentum of the instability of the Myers-Perry black hole. The bumpy black hole construction and perturbation analysis of the Myers-Perry black hole had been investigated numerically. These numerical studies of the solution and perturbations need very advanced and sophisticated technique. However the effective theory obtained in this paper is rather simple equation and we can obtain the solution easily.

As another application we have obtained the quasinormal mode frequencies of the singly rotating Myers-Perry black hole. Our effective theory is only for the stationary black hole. But, if we consider the dynamics with $\omega r_0 = O(D^0)$, the time-dependence becomes sub-dominant compared with the radial dynamics. As a result we could solve the perturbation equation as the ordinarily differential equation with respect to the radial direction. Furthermore the leading order solution of our effective theory has a very important

JHEP09(2015)193

property, the boost property. All stationary black hole solution is represented as the boost transformation of the Schwarzschild black hole. Thus various things which Schwarzschild black hole possess are common with stationary black holes. Using this useful feature we have solved the perturbation equation of the singly rotating Myers-Perry black hole explicitly and obtained the quasinormal mode condition, which is just an algebraic equation, analytically. Although originally the perturbation equation is the partial differential equation system, the large radial gradient and boost property of the large D Myers-Perry black hole reduce the equation to the analytically solvable ordinarily differential equation.

We can consider many directions of the extension of our work. In this paper we consider the solution with only one angular momentum in vacuum. Thus it is interesting to include more angular momentum, matter fields such as a gauge field or some compact dimensions into the effective theory of stationary black holes. These inclusions would give further additional degree of freedom for the deformation of the horizon. So its dynamics becomes much richer. Another direction of the extension is the more detail investigation of the effective theory of stationary black hole by searching other solution such as black ring solutions and going to more higher order nonlinear solutions. By constructing such solution we can draw the phase diagram of black holes analytically and compare with numerical results. Actually the higher order investigation of the effective theory for the static solution [9] allows very interesting phenomena such as the existence of the critical dimension of the non-uniform black string [36].

Acknowledgments

The authors are very grateful to Roberto Emparan and Hideo Kodama for valuable comments on the draft and useful discussions. KT was supported by JSPS Grant-in-Aid for Scientific Research No.26-3387.

A Singly rotating AdS Myers-Perry black hole

In this appendix we give the metric of the AdS Myers-Perry black hole and its large D limit in our notation. The $D = n + 3$ dimensional singly rotating AdS Myers-Perry black hole is given by [15, 16][13]

$$\begin{aligned} ds^2 = &-A(r,\theta)^2 dt^2 + B(r,\theta)^2 d\hat{\mathsf{R}}^2 + F(r,\theta)^2 (d\phi - w(r,\theta)dt)^2 \\ &+ G(r,\theta)^2 d\theta^2 + r^2 \cos^2\theta d\Omega_{D-4}^2, \end{aligned} \tag{A.1}$$

where

$$A(r,\theta)^2 = \frac{\Delta_{\hat{\mathsf{R}}}\Delta_\theta (r^2+L^2)(r^2+a^2\cos^2\theta)}{L^2\Xi\Delta_{\hat{\mathsf{R}}}(r^2+a^2\cos^2\theta) + r^2L^2\Delta_\theta(r^2+a^2)}, \tag{A.2}$$

[13] We change the ϕ coordinate by

$$\phi \to \phi - \frac{a}{L^2}dt$$

from [15, 16] to satisfy the boundary condition (2.13).

JHEP09(2015)193

$$B(r,\theta)^2 = \frac{r^2}{n^2\hat{\mathsf{R}}^2}\frac{\hat{\mathsf{R}}(r^2+a^2\cos^2\theta)}{\Delta_{\hat{\mathsf{R}}}}, \tag{A.3}$$

$$F(r,\theta)^2 = \sin^2\theta\left(\frac{r^2+a^2}{\Xi}+\frac{a^2r^2\sin^2\theta}{\Xi^2(r^2+a^2\cos^2\theta)\hat{\mathsf{R}}}\right), \tag{A.4}$$

$$w(r,\theta) = \frac{ar^2\Delta_\theta}{L^2\Xi\Delta_{\hat{\mathsf{R}}}(r^2+a^2\cos^2\theta)+r^2L^2\Delta_\theta(r^2+a^2)}, \tag{A.5}$$

and

$$G(r,\theta)^2 = \frac{r^2+a^2\cos^2\theta}{\Delta_\theta}. \tag{A.6}$$

Here we defined

$$\hat{\mathsf{R}} = \left(\frac{r}{r_0}\right)^n, \qquad \Xi = 1-\frac{a^2}{L^2}, \tag{A.7}$$

and following functions

$$\Delta_{\hat{\mathsf{R}}} = r^2-(r^2+a^2)\left(1+\frac{r^2}{L^2}\right)\hat{\mathsf{R}}, \qquad \Delta_\theta = 1-\frac{a^2}{L^2}\cos^2\theta. \tag{A.8}$$

The horizon position, $r=r_+$, is defined by the positive real root of $\Delta_{\hat{\mathsf{R}}}$ by

$$\Delta_{\hat{\mathsf{R}}}(r_+) = 0. \tag{A.9}$$

L is the AdS curvature and the metric is the solution of the Einstein equation with a cosmological constant

$$\Lambda = -\frac{(D-1)(D-2)}{L^2}. \tag{A.10}$$

At the large D limit the metric is simplified to[14]

$$\begin{aligned} ds^2 = {} & \frac{d\mathsf{R}^2}{n^2}\frac{L^2(1+a^2\cos^2\theta)}{(1+a^2)(1+L^2)\mathsf{R}(\mathsf{R}-1)} \\ & -\left(1-\frac{\cosh^2\sigma(\theta)}{\mathsf{R}}\right)d\hat{t}^2+\left(1+\frac{\sinh^2\sigma(\theta)}{\mathsf{R}}\right)d\hat{\phi}^2 \\ & -\frac{2\sinh\sigma(\theta)\cosh\sigma(\theta)}{\mathsf{R}}d\hat{t}\;d\hat{\phi}+\frac{1+a^2\cos^2\theta}{\Delta_\theta}d\theta^2+\cos^2\theta d\Omega_{D-4}^2, \end{aligned} \tag{A.11}$$

where we introduced

$$\mathsf{R} = \frac{(1+a^2)(1+L^2)}{L^2}\hat{\mathsf{R}}, \qquad \cosh^2\sigma(\theta) = \frac{(1+a^2)\Delta_\theta}{(1+a^2\cos^2\theta)\Xi}. \tag{A.12}$$

$d\hat{t}$ and $d\hat{\phi}$ are defined by

$$d\hat{t}^2 = \frac{(1+L^2)\Delta_\theta}{L^2\Xi}dt^2, \qquad d\hat{\phi}^2 = \frac{1+a^2}{\Xi}\sin^2\theta d\phi^2. \tag{A.13}$$

[14] In the following we set $r_0=1$.

JHEP09(2015)193

At the large D limit the horizon is located on

$$\mathsf{R}\Big|_{r=r_+} = 1 + O(1/n). \tag{A.14}$$

This solution can be reproduced by the leading order solution in section 2 by

$$\mathsf{V}_0(\theta)^2 = \frac{(1+L^2)\Delta_\theta}{L^2\Xi}, \qquad \mathcal{R}_{\rm H}(z) = \cos\theta, \tag{A.15}$$

and

$$\frac{dz}{d\theta} = \sqrt{\frac{1+a^2\cos^2\theta}{\Delta_\theta}}, \qquad \mathsf{R} = \cosh^2\rho. \tag{A.16}$$

The surface gravity and horizon angular velocity at the leading order of large D limit are

$$\hat{\kappa} = \frac{1}{2}\frac{1+L^2}{L^2}, \qquad \Omega_H = \frac{a}{1+a^2}\frac{1+L^2}{L^2}. \tag{A.17}$$

The metric (A.11) becomes the large D metric of the Schwarzschild black hole [3]

$$ds^2 = \frac{4}{n^2}d\rho^2 - \tanh^2\rho\, dt^2 + dz^2 + \sin^2\theta d\phi^2 + \cos^2\theta d\Omega^2_{D-4}, \tag{A.18}$$

when $a = 0$ and $1/L = 0$. We changed the coordinate by $\mathsf{R} = \cosh^2\rho$.

Structure in $1/D$ correction. Let us consider the $1/D$ correction in g_{tt} of the AdS Myers-Perry black hole at $a = 0$. Using

$$r = 1 + \frac{\log\hat{\mathsf{R}}}{n} + O(1/n^2) \tag{A.19}$$

we find that g_{tt} becomes

$$\begin{aligned} g_{tt} &= -A(r,\theta)^2 \\ &= 1 + \frac{1}{L^2} - \frac{1}{\hat{\mathsf{R}}} + \frac{2\log\hat{\mathsf{R}}}{nL^2} + O(1/n^2). \end{aligned} \tag{A.20}$$

At large R g_{tt} has a linear term in ρ since the relation between ρ and $\hat{\mathsf{R}}$ is

$$\hat{\mathsf{R}} = \frac{L^2}{1+L^2}\cosh^2\rho. \tag{A.21}$$

Thus, in general, the higher order corrections in $A(\rho,\theta)$ cannot be assumed to be damping exponentially at the overlap region $n \gg \rho \gg 1$ in the presence of the cosmological constant as mentioned in section 2.

JHEP09(2015)193

A.1 Ellipsoidal embedding

The AdS-Myers-Perry black hole is described as the solution of the effective equation (2.39) for the ellipsoidal embedding in the AdS background. The ellipsoidal coordinate in AdS is given by[15]

$$ds^2 = -\frac{\Delta_\theta(L^2+r^2)}{L^2\Xi}dt^2 + \frac{L^2(r^2+a^2\cos^2\theta)}{(r^2+a^2)(L^2+r^2)}dr^2 + \frac{r^2+a^2\cos^2\theta}{\Delta_\theta}d\theta^2 + \frac{(r^2+a^2)\sin^2\theta}{\Xi}d\phi^2 + r^2\cos^2\theta d\Omega_{D-4}^2. \tag{A.22}$$

The ellipsoidal embedding is defined by

$$r = r(\theta) = \frac{\mathcal{R}_{\rm H}(\theta)}{\cos\theta}, \tag{A.23}$$

and the leading order metric of the AdS Myers-Perry black hole in the $1/D$ expansion is reproduced by $r(\theta) = 1$ when we fix the horizon position by $r_+ = 1$ with the surface gravity and horizon angular velocity given in eq. (A.17). We consider the perturbation around this AdS Myers-Perry black hole embedding. As done in section 2 the obtained perturbed solution would give the bumpy black hole solution in AdS in the perturbative manner. At first we fix the surface gravity to

$$\hat{\kappa} = \frac{1+L^2}{2L^2}, \tag{A.24}$$

by using the time coordinate normalization in near zone. The perturbed embedding is

$$\mathcal{R}_{\rm H}(\theta) = \cos\theta\Big[1 + \epsilon\hat{\mathcal{R}}(\theta) + O\left(\epsilon^2\right)\Big], \tag{A.25}$$

where

$$\epsilon = \Omega_H - \frac{a}{1+a^2}\frac{1+L^2}{L^2}. \tag{A.26}$$

Then, perturbing eq. (2.39) with respect to ϵ, we find the perturbative solution

$$\hat{\mathcal{R}}(\theta) = \frac{a(1+a^2)^2\sin^2\theta}{\Xi(1-a^2)(1+a^2\cos^2\theta)} + A\frac{(\sin\theta)^{\delta_{\rm MP}}\Delta_\theta^{1-\delta_{\rm MP}/2}}{1+a^2\cos^2\theta}, \tag{A.27}$$

where

$$\delta_{\rm MP} = \frac{(1+a^2)(L^2-1)}{L^2\Xi}. \tag{A.28}$$

This perturbation solution becomes regular at $\theta = 0$ when $a = a_c$ given by

$$a_c^2 = \frac{(2k-1)L^2+1}{L^2+2k-1} \tag{A.29}$$

[15]The coordinate transformation from the usual AdS coordinate to the ellipsoidal coordinate is [15]

$$r^2\sin^2\theta \to \Xi^{-1}(r^2+a^2)\sin^2\theta, \qquad r^2\cos^2\theta \to r^2\cos^2\theta.$$

JHEP09(2015)193

where k is a positive integer. At $L \to \infty$ eq. (A.29) reproduces the threshold angular momentum (2.56). Hence we expect that eq. (A.29) gives the threshold angular momentum of the AdS Myers-Perry black hole and branching angular momentum for the bumpy black hole in AdS. It is interesting to check this result by solving the perturbation equation of the AdS Myers-Perr black hole and obtaining the QNM frequency as done for the Myers-Perry black hole in section 4.

B Next-to-leading order analysis

Here we briefly give results for next-to-leading order solutions. In particular we will see how the constancy condition of the surface gravity and horizon angular velocity, eq. (2.30), can be obtained.

Our $D = n + 3$ dimensional metric ansatz is

$$\begin{aligned} ds^2 = &\frac{N^2(\rho,z)}{n^2}d\rho^2 - A(\rho,z)^2dt^2 + F(\rho,z)^2(d\phi - W(\rho,z)dt)^2 \\ &+ G(\rho,z)^2dz^2 + H(\rho,z)^2 q_{AB}dx^A dx^B. \end{aligned} \tag{B.1}$$

We solve the Einstein equations for metric functions and the extrinsic curvature on $\rho =$ constant surface defined by

$$K^a{}_b = \frac{n}{2N(\rho,z)} g^{ac}\partial_\rho g_{cb}. \tag{B.2}$$

The Einstein equations are decomposed on $\rho =$ constant surface as

$$-R + K^2 - K^a{}_b K^b{}_a - \frac{(D-1)(D-2)}{L^2} = 0, \tag{B.3}$$

$$\nabla_a K^a{}_b - \nabla_b K = 0, \tag{B.4}$$

$$\frac{n}{N}\partial_\rho K^a{}_b = -KK^a{}_b + R^a{}_b + \frac{D-1}{L^2}\delta^a{}_b - \frac{1}{N}\nabla^a\nabla_b N. \tag{B.5}$$

The leading order solutions which are regular on the horizon are

$$A(\rho,z)^2 = \frac{A_0(z)^2F_0(z)^2\tanh^2\rho}{F_0(z)^2 - A_0(z)^2C_{t\phi}(z)^2\tanh^2\rho}, \tag{B.6}$$

$$F(\rho,z)^2 = F_0(z)^2 - A_0(z)C_{t\phi}(z)^2\tanh^2\rho, \tag{B.7}$$

$$W(\rho,z) = \frac{F_0(z)^2(1-C_{tt}(z)) + A_0(z)^2C_{t\phi}(z)^2C_{tt}(z)\tanh^2\rho}{K_{t\phi}(z)F_0(z)^2 - A_0(z)^2C_{t\phi}(z)^3\tanh^2\rho}, \tag{B.8}$$

and

$$G(\rho,z) = 1 - \frac{2r_0(z)^2}{n}\left(\frac{\mathcal{R}_{\rm H}''(z)}{\mathcal{R}_{\rm H}(z)} - \frac{1}{L^2}\right)\log(\cosh\rho), \tag{B.9}$$

$$H(\rho,z) = \mathcal{R}_{\rm H}(z)\left(1 + \frac{2}{n}\log(\cosh\rho)\right). \tag{B.10}$$

JHEP09(2015)193

To satisfy the boundary conditions at $\rho \gg 1$, C_{tt} and $C_{t\phi}$ are found to be

$$C_{tt}(z) = \frac{1}{A_0(z)^2} \quad C_{t\phi}(z) = \frac{F_0(z)\sqrt{1-A_0(z)^2}}{A_0(z)}. \tag{B.11}$$

Then we can see that the leading order solutions satisfy the boundary condition at $\rho \gg 1$ as

$$A(\rho, z) = 1 + O(e^{-\rho}), \qquad W(\rho, z) = O(e^{-\rho}). \tag{B.12}$$

Furthermore the functions in this leading order solution should satisfy one equation coming from the vector constraint (B.4) given by

$$\frac{d}{dz}\log\left(\frac{A_0(z)C_{tt}(z)}{r_0(z)}\right) - (1 - C_{tt}(z))\frac{d}{dz}\log\left(\frac{C_{tt}(z)}{C_{t\phi}(z)}\right) = 0. \tag{B.13}$$

This equation is rewritten by using eq. (B.11) as

$$\frac{d}{dz}\log\left(A_0 r_0(z)\right) + \frac{1-A_0(z)^2}{A_0(z)^2}\frac{d}{dz}\log\left(A_0(z)F_0(z)\sqrt{1-A_0(z)^2}\right) = 0. \tag{B.14}$$

We consider the $1/D$ corrections to the leading order solutions. Especially, by solving eq. (B.5), we found that the $1/D$ correction to $K^z{}_z$, say ${}^{(1)}K^z{}_z$, has the following form

$${}^{(1)}K^z{}_z = \frac{C^{(1)}_{zz}}{\sinh\rho} + \delta K^z{}_z(\rho, z), \tag{B.15}$$

where $C^{(1)}_{zz}$ is an integration function with respect to ρ-integration. $\delta K^z{}_z(\rho, z)$ is a solution coming from the integration of the source term at next-to-leading order. $C^{(1)}_{zz}$ is used to eliminate the divergence of $O(\rho^{-1})$ in $\delta K^z{}_z(\rho, z)$ at the horizon $\rho = 0$. Even though the $O(\rho^{-1})$ divergence is eliminated by the integration function, ${}^{(1)}K^z{}_z$ cannot satisfy the regularity condition at the horizon. Actually $\delta K^z{}_z(\rho, z)$ has the following behavior after eliminating $O(\rho^{-1})$ divergence at the horizon

$$\begin{aligned}\delta K^z{}_z(\rho, z) = &-\frac{r_0(z)\log\rho}{(1-A_0(z)^2)A_0(z)^2F_0(z)^2\rho} \\ &\times\left[F_0(z)A_0'(z) + (1-A_0^2)A_0(z)F_0'(z)\right]^2 + O(1).\end{aligned} \tag{B.16}$$

To satisfy the regularity condition on the horizon we should eliminate also this $O(\rho^{-1}\log\rho)$ divergence. Then $A_0(z)$ and $F_0(z)$ should satisfy additional condition

$$F_0(z)A_0'(z) + (1-A_0^2)A_0(z)F_0'(z) = 0. \tag{B.17}$$

This condition can be solved by

$$F_0(z) = \frac{\sqrt{1-A_0(z)^2}}{\Omega_{\rm H}A_{0(z)}}, \tag{B.18}$$

where we introduce an integration constant $\Omega_{\rm H}$. Using this solution (B.18), eq. (B.14) is reduced to the equation only for $A_0(z)$, and it can be solved by

$$A_0(z) = 2\hat{\kappa}r_0(z), \tag{B.19}$$

where $\hat{\kappa}$ is an integration constant.

JHEP09(2015)193

Let us summarize above results. We obtained additional condition (B.17) from the boundary condition on $O(1/D)$ corrections. By combining this additional condition with the leading order vector constraint (B.14) we get the expressions of $A_0(z)$ and $F_0(z)$ in terms of $r_0(z)$ and integration constants as eqs. (B.18) and (B.19). Using eq. (B.11) we can see that eq. (2.30) is obtained by defining $\kappa = n\hat{\kappa}$.

C Spheroidal harmonics at large D

We give some analysis for the spheroidal harmonics in the $1/D$ expansion. Let us consider the massless scalar field equation

$$\Box\Psi = 0, \tag{C.1}$$

in the $D = n + 3$ dimensional flat spacetime in the ellipsoidal coordinate given by

$$\begin{aligned} ds^2 = &-dt^2 + \frac{r^2 + a^2\cos^2\theta}{r^2 + a^2}dr^2 + (r^2 + a^2\cos^2\theta)d\theta^2 \\ &+ (r^2 + a^2)\sin^2\theta d\phi^2 + r^2\cos^2\theta d\Omega^2_{D-4}. \end{aligned} \tag{C.2}$$

a is an oblateness parameter. The scalar field can be decomposed as

$$\Psi = e^{-i\omega t}e^{im\phi}\psi(r)S(\theta)\mathbb{Y}_j. \tag{C.3}$$

$\mathbb{Y}_j$ is the spherical harmonics on S^{D-4} with the angular momentum number j. Eq. (C.1) becomes equations for $\psi(r)$ and $S(\theta)$ as

$$\left[\frac{1}{r^{n-1}}\partial_r r^{n-1}\partial_r + \frac{((r^2+a^2)\omega + am)^2}{r^2+a^2} - \frac{a^2(j(j+n-2))}{r^2} - \Lambda\right]\psi(r) = 0, \tag{C.4}$$

and

$$\left[\frac{1}{\sin\theta\cos^{n-1}\theta}\partial_\theta \sin\theta\cos^{n-1}\theta\partial_\theta - \frac{(a\omega\sin^2\theta + m)^2}{\sin^2\theta} - \frac{j(j+n-2)}{\cos^2\theta} + \Lambda\right]S(\theta) = 0. \tag{C.5}$$

Λ is the separation constant. The spheroidal harmonics, $S(\theta)$, is defined by the solution of eq. (C.5). While there are numerical analysis [37] to find solution and eigenvalue of eq. (C.5), but it is hard to obtain analytic solutions of eq. (C.5). Here we apply the large D expansion to solve eq. (C.5). At first we assume that the parameters in eq. (C.5) have following orders at large D

$$\omega = O(1), \qquad a = O(1), \qquad m = O(1), \qquad j = O(1), \qquad \Lambda = O(n). \tag{C.6}$$

The reason for $\Lambda = O(n)$ can be seen by considering $a = 0$ limit. At $a = 0$ eq. (C.5) is reduced to the equation for the spherical harmonics. The equation at $a = 0$ can be solved by $S_\ell^{(a=0)}(\theta)$

$$S^{(a=0)}(\theta) = \cos^j\theta\ \sin^{|m|}\theta\ {}_2F_1(-k_S, k_S + |m| + j + n/2, |m| + 1; \sin^2\theta), \tag{C.7}$$

JHEP09(2015)193

with the separation constant

$$\Lambda^{(a=0)} = \ell(\ell + n). \tag{C.8}$$

k_S is given by

$$k_S = \frac{\ell - j - |m|}{2}. \tag{C.9}$$

Then, at $a = 0$, the separation constant is $O(n)$. The spheroidal harmonics becomes the spherical harmonics at $a = 0$. Thus it is natural to assume $\Lambda = O(n)$ also at $a \neq 0$. The important observation is that the spherical harmonics (C.7) has the following large D behaviors

$$S_\ell^{(a=0)}(\theta) = \sin^{\ell-j}\theta \cos^j\theta + O(1/n). \tag{C.10}$$

Usually the spherical harmonics $S_\ell^{(a=0)}(\theta)$ is understood as the function which has ℓ nodes. This ℓ is the overtone number along θ direction. At large D limit the situation is changed, and any nodes would disappear according to the large D limit solution (C.10). Instead the quantum number ℓ can be read from the behavior only around $\theta = 0$ as the degree of vanishing as

$$S_\ell^{(a=0)}(\theta) = \theta^\ell \left(1 + O(\theta, n^{-1})\right). \tag{C.11}$$

Although it is not still unclear why we can obtain the quantum number ℓ only by the behavior around $\theta = 0$, not by the behavior both at $\theta = 0$ and $\theta = \pi/2$, such behavior is useful for the quasinormal mode analysis of the Myers-Perry black hole.

Next we consider the contributions by $a \neq 0$ to the spheroidal harmonics. Let us assume that the spheroidal harmonics $S(\theta)$ is modified by the contributions from a and ω as

$$S(\theta) = S_\ell^{(a=0)}(\theta)\left(1 + \delta S(\theta)\right). \tag{C.12}$$

Substituting this into eq. (C.5) and linearizing the equation with respect to $\delta S(\theta)$, we can obtain the equation for $\delta S(\theta)$. The obtained equation, however, does not have a and ω dependences in its equation at the leading order of the large D limit. This is because the contributions of a and ω are not leading order effects in eq. (C.5) in the $1/D$ expansion. Thus $\delta S(\theta)$ can be set to zero also for the spheroidal harmonics $S(\theta)$ at the leading order in the $1/D$ expansion. Hence the spheroidal harmonics has the following large D form

$$\begin{aligned} S(\theta) &= S_\ell^{(a=0)}(\theta) + O(1/n) \\ &= \sin^{\ell-j}\theta \cos^j\theta + O(1/n), \end{aligned} \tag{C.13}$$

and the separation constant also becomes

$$\Lambda = \ell n \left(1 + O(n^{-1})\right), \tag{C.14}$$

where ℓ is non-negative integer. The quantum number along θ direction, ℓ, can be obtained again only by the behavior around $\theta = 0$. If one considers the $1/D$ corrections to the spheroidal harmonics we can obtain the $1/D$ correction to the separation constant. In the analysis of this paper we consider only the leading order results of the quasinormal modes, so we do not pursue this analysis in more detail here.

JHEP09(2015)193

D Detail analysis on the vector type perturbation

In this appendix we show the detail analysis of the vector type perturbation of the Myers-Perry- black hole. The vector type perturbation on the Myers-Perry black hole is decomposed to

$$h^{(V)}_{\mu\nu}dx^\mu dx^\nu = e^{-i\omega t}e^{im\phi}\Big[f_I^{(V)\mathrm{Sch}}\mathbb{Y}_A^{(V)j}e^{(I)}e^{(A)} + H_L^{(V)}\mathbb{Y}_{AB}^{(V)j}e^{(A)}e^{(B)}\Big], \tag{D.1}$$

where the vielbein and the vector harmonics were defined in section 3. The decoupling perturbation variables are defined by

$$F_0^{(V)} = \frac{\cosh\rho}{\sqrt{1+r_0(z)^2\sinh^2\rho}}f_0^{(V)} - \sinh\rho\sqrt{\frac{1-r_0(z)^2}{1+r_0(z)^2\sinh^2\rho}}f_2^{(V)}, \tag{D.2}$$

$$F_2^{(V)} = \frac{\cosh\rho}{\sqrt{1+r_0(z)^2\sinh^2\rho}}f_2^{(V)} - \sinh\rho\sqrt{\frac{1-r_0(z)^2}{1+r_0(z)^2\sinh^2\rho}}f_0^{(V)}, \tag{D.3}$$

and

$$F_1^{(V)} = f_1^{(V)}, \qquad F_3^{(V)} = f_3^{(V)}, \qquad F_L^{(V)} = H_L^{(V)}. \tag{D.4}$$

The decoupling perturbation variables are expanded by

$$F_I^{(V)} = \sum_{k\geq 0}\frac{{}^{(k)}F_I^{(V)}}{n^k},\ F_{T,L}^{(V)} = \sum_{k\geq 0}\frac{{}^{(k)}F_L^{(V)}}{n^k}. \tag{D.5}$$

Changing coordinate by $\mathsf{R} = \cosh^2\rho$, the perturbation equation at each order becomes

$$\frac{\partial}{\partial\mathsf{R}}\mathsf{R}(\mathsf{R}-1)\frac{\partial}{\partial\mathsf{R}}{}^{(k)}F_0^{(V)} - \frac{{}^{(k)}F_0^{(V)}}{4\mathsf{R}(\mathsf{R}-1)} = {}^{(k)}\mathcal{S}_0^{(V)}, \tag{D.6}$$

$$\frac{\partial}{\partial\mathsf{R}}\mathsf{R}(\mathsf{R}-1)\frac{\partial}{\partial\mathsf{R}}{}^{(k)}F_1^{(V)} - \frac{{}^{(k)}F_1^{(V)}}{4\mathsf{R}(\mathsf{R}-1)} = {}^{(k)}\mathcal{S}_1^{(V)}, \tag{D.7}$$

$$\frac{\partial}{\partial\mathsf{R}}\mathsf{R}(\mathsf{R}-1)\frac{\partial}{\partial\mathsf{R}}{}^{(k)}F_2^{(V)} = {}^{(k)}\mathcal{S}_2^{(V)}, \tag{D.8}$$

$$\frac{\partial}{\partial\mathsf{R}}\mathsf{R}(\mathsf{R}-1)\frac{\partial}{\partial\mathsf{R}}{}^{(k)}F_3^{(V)} = {}^{(k)}\mathcal{S}_3^{(V)}. \tag{D.9}$$

The boundary condition is the same with one of the scalar type perturbation, the ingoing boundary condition on the horizon (4.4) and decoupling mode condition (4.5) at asymptotic infinity of near zone.

Leading order ($k = 0$). The regular solution at the leading order is

$${}^{(0)}F_0^V = {}^{(0)}F_1^V = \frac{W_{(0)}}{\sqrt{\mathsf{R}(\mathsf{R}-1)}}, \qquad {}^{(0)}F_2^V = {}^{(0)}F_3^V = 0. \tag{D.10}$$

The leading order solution has an undetermined function $W_{(0)}$ by the boundary condition.

JHEP09(2015)193

Next-to leading order ($k = 1$). The regular solution at the next to leading order is

$$ {}^{(1)}F_0^V = \frac{W_{(1)}}{\sqrt{\mathsf{R}(\mathsf{R}-1)}} + {}^{(1)}\hat{F}_0^V, \ {}^{(1)}F_1^V = \frac{W_{(1)}}{\sqrt{\mathsf{R}(\mathsf{R}-1)}} + {}^{(1)}\hat{F}_1^V, \tag{D.11} $$

and

$$ {}^{(0)}F_2^V = {}^{(1)}\hat{F}_2^V, \ {}^{(0)}F_3^V = {}^{(1)}\hat{F}_3^V, \tag{D.12} $$

where terms with the hat come from the integrations of source terms. The next to leading order solution has an undetermined function $W_{(1)}$ by the boundary condition again. At this order we obtain the non-trivial condition for $W_{(0)}$ as

$$ \begin{aligned} &\cos\theta \sin^2\theta (1 + a^2\cos^2\theta) W'_{(0)}(\theta) \\ &\quad + \Big[-j(1 + a^2\cos^2\theta) + i\cos^2\theta (a^4 \cos^2\theta(\omega - i) - a^3 m \cos^2\theta \\ &\qquad + a^2(\cos^2\theta(\omega + i) + \omega - 2i) + \omega - am) \Big] W_0(\theta) = 0. \end{aligned} \tag{D.13} $$

This condition can be solved explicitly as

$$ W_{(0)}(\theta) = \frac{\cos^j\theta \sin^{{}^{(0)}\delta_\omega^V}\theta}{1 + a^2\cos^2\theta}, \tag{D.14} $$

where

$$ {}^{(0)}\delta_\omega^V = -(1 + a^2)(j - 1) - iam + i(1 + a^2)\omega. \tag{D.15} $$

The harmonics condition on $W_0(\theta)$ is eq. (4.18) as

$$ {}^{(0)}\delta_\omega^V = \ell - j, \tag{D.16} $$

and ℓ is parameterized by the non-negative integer k_V by

$$ \ell = j + |m| + 2k_V. \tag{D.17} $$

This harmonics condition gives the leading order QNM frequency for the vector type perturbation by

$$ \omega_{\mathrm{LO}}^V = \frac{am}{1 + a^2} - i\left(j - 1 + \frac{\ell - j}{1 + a^2} \right). \tag{D.18} $$

Next-to-next-to leading order. At this order we can obtain the solution and undetermined function in the same manner. Furthermore we find the non-trivial condition on $W_{(1)}(\theta)$. Although we omit the explicit form of it since it is not so illuminative, the solution of the non-trivial condition gives the following behavior around $\theta = 0$ on the horizon $\mathsf{R} = 1$

$$ F_{(0)}^V = \frac{\theta^{\delta_\omega^V}}{\sqrt{\mathsf{R} - 1}}(1 + O(\theta, 1/n^2)) \tag{D.19} $$

JHEP09(2015)193

where

$$\delta^V_\omega = {}^{(0)}\delta^V_\omega + \frac{{}^{(1)}\delta^V_\omega}{n}. \tag{D.20}$$

${}^{(0)}\delta^V_\omega$ is given in eq. (D.15). ${}^{(1)}\delta^V_\omega$ is

$$\begin{aligned}{}^{(1)}\delta^V_\omega = {} & a^2(-a^2(j-1)^2 + 2ia(j-1)m + j^2 - 2j - m^2 + 1) \\ & - a(2a(j-1) + im\log(1+a^2)) + \omega(i(a^2-1)\log(1+a^2) \\ & + 2ia^2(a^2(j-1) + iam + j - 1)) + (1+a^2)^2\omega^2.\end{aligned} \tag{D.21}$$

Then the harmonics condition gives

$${}^{(0)}\delta^V_\omega + \frac{{}^{(1)}\delta^V_\omega}{n} = \ell - j. \tag{D.22}$$

This condition is solved by

$$\omega^V = \omega^V_{\rm LO} + \frac{\omega^V_{\rm NLO}}{n} + O(1/n^2), \tag{D.23}$$

where

$$\begin{aligned}\omega^V_{\rm NLO} = {} & \frac{2am}{1+a^2}\Big(\ell - 1 + a^2(j-1) + \log(1+a^2)\Big) \\ & - i\Bigg((j-1)^2 + \frac{(1+a^2)(\ell-j)(\ell+j-2) - 2a^2m^2}{(1+a^2)^2} \\ & + \left(j - 1 - \frac{\ell-j}{1+a^2} + \frac{2(\ell-j)}{(1+a^2)^2}\right)\log(1+a^2)\Bigg).\end{aligned} \tag{D.24}$$

E Explicit forms of $c_i(\theta)$ and $d_i(\theta)$

The scalar type perturbation can satisfy the boundary condition on the horizon at the next to next to the leading order if the integration functions are solutions of following equations:

$$\begin{aligned}& c_1(\theta)C''_{(1)}(\theta) + c_2(\theta)C'_{(1)}(\theta) + c_3(\theta)C_{(1)}(\theta) \\ & \quad + c_4(\theta)D''_{(0)}(\theta) + c_5(\theta)D'_{(0)}(\theta) + c_6(\theta)D_{(0)}(\theta) = 0,\end{aligned} \tag{E.1}$$

and

$$\begin{aligned}& d_1(\theta)D'''_{(0)}(\theta) + d_2(\theta)D''_{(0)}(\theta) + d_3(\theta)D'_{(0)}(\theta) \\ & \quad + d_4(\theta)D_{(0)}(\theta) + d_5(\theta)C'_{(1)}(\theta) + d_6(\theta)C_{(1)}(\theta) = 0.\end{aligned} \tag{E.2}$$

Each coefficients are following:

$$c_1(\theta) = \frac{\cos^2\theta\sin^3\theta\left(1 + a^2\cos\theta^2\right)}{2\left(1+a^2\right)^{5/2}}, \tag{E.3}$$

JHEP09(2015)193

$$
\begin{aligned}
c_2(\theta) = {} & \frac{\cos\theta \sin^2\theta}{2\left(1+a^2\right)^{5/2}}\Big[2a^2\cos^4\theta\left(a^2(j-i\omega)+iam-i\omega+2\right) \\
& +\cos^2\theta\left(a^2(4j-2i\omega-5)+2iam-2i\omega-2\right)+2j+1\Big], \qquad \text{(E.4)} \\
c_3(\theta) = {} & \frac{\sin^2\theta}{2\left(1+a^2\right)^{5/2}}\Big[a^2\cos^6\theta\left(a^2(j-i\omega)+iam-i\omega+2\right)^2 \\
& +\cos^2\theta\left(a^2\left(3j^2+j(-4-2i\omega)-1\right)+2iajm+j(-4-2i\omega)+4\right) \\
& +\cos^4\theta\Big(a^4\left(3j^2+j(-6-4i\omega)-\omega^2+6i\omega+4\right)+2a^3m(2ij+\omega-3i) \\
& -a^2\left(m^2+2\left(2i(j-2)\omega+\omega^2-1\right)\right)+2am(\omega-i)-\omega(\omega-2i)\Big) \\
& +j^2+2j-3\Big], \qquad \text{(E.5)} \\
c_4(\theta) = {} & -\frac{\sin^2\theta}{\left(1+a^2\right)^4\cos\theta}\Big[\cos^2\theta\left(a^2(-5j+3i\omega+2)-3iam+j+3i\omega+5\right) \\
& +\cos^4\theta\left(a^4(-2j+3i\omega+3)-3ia^3m+a^2(j+2i\omega+1)-i\omega\right) \\
& -ia^2\left(1+a^2\right)\omega\cos^6\theta-3j-5\Big], \qquad \text{(E.6)} \\
c_5(\theta) = {} & \frac{\sin\theta}{\left(1+a^2\right)^4\cos^2\theta\left(1+a^2\cos^2\theta\right)}\Big[\cos^2\theta\Big(a^2\left(10j^2+2j(8-3i\omega)-7i\omega-3\right) \\
& +ia(6j+7)m-2j^2+j(-19-6i\omega)-7i\omega-9\Big) \\
& +a^4\left(a^2+1\right)\omega\cos^{10}\theta\left(a^2(2ij+2\omega-i)-2am+2\omega+3i\right) \\
& +\cos^4\theta\Big(a^4\left(12j^2+j(-6-16i\omega)-3\omega^2-i\omega-9\right)+a^3m(16ij+6\omega+i) \\
& -a^2\left(6j^2+4j(7+3i\omega)+3m^2+6\omega^2-9i\omega+2\right) \\
& +am(-2ij+6\omega-9i)+j(5+4i\omega)-3\omega^2+10i\omega+4\Big) \\
& +a^2\cos^8\theta\Big(a^6\left(j^2+j(-3-4i\omega)-3\omega^2+4i\omega+2\right)+2a^5m(2ij+3\omega-2i) \\
& -a^4\left(2j^2+j(-2-4i\omega)+3m^2+2\omega(\omega+i)\right)+a^3m(-2ij+2\omega+i) \\
& +a^2\left(8ij\omega+j+5\omega^2-5i\omega-2\right)+am(-4\omega+i)+\omega(4\omega+i)\Big) \\
& +\cos^6\theta\Big(a^6\left(6j^2+j(-12-14i\omega)-6\omega^2+10i\omega+5\right)+2a^5m(7ij+6\omega-5i) \\
& -a^4\left(6j^2+j(7+4i\omega)+6m^2+10\omega^2-15i\omega-15\right)+2a^3m(-2ij+5\omega-4i) \\
& +a^2\left(2j(3+5i\omega)-2\omega^2+3i\omega+6\right)+am(-2\omega+i)+2\omega(\omega-i)\Big) \\
& +3j^2+13j+5\Big], \qquad \text{(E.7)} \\
d_1(\theta) = {} & -\frac{\cos\theta\sin^3\theta}{\left(1+a^2\right)^2\left(1+a^2\cos^2\theta\right)}, \qquad \text{(E.8)} \\
d_2(\theta) = {} & -\frac{\sin^2\theta}{\left(1+a^2\right)^2\left(1+a^2\cos^2\theta\right)^2}\Big[3j+1+\cos^2\theta\left(a^2(6j-3i\omega-4)+3iam-3i\omega-1\right) \\
& +a^2\cos^4\theta\left(3a^2(j-i\omega-1)+3iam-3i\omega+1\right)\Big], \qquad \text{(E.9)}
\end{aligned}
$$

JHEP09(2015)193

$$
\begin{aligned}
d_3(\theta) = &-\frac{\sin\theta}{(1+a^2)^2\cos\theta\,(1+a^2\cos^2\theta)^3}\Big[\cos^2\theta\Big(a^2\left(12j^2-6ij\omega+j+i\omega+3\right)\\
&+ia(6j-1)m-6ij\omega-6j+i\omega-1\Big)+a^4\cos^8\theta\Big(a^4\left(3j^2-6ij\omega-4j-3\omega^2+5i\omega+2\right)\\
&+a^3m(6ij+6\omega-5i)+a^2\left(-6ij\omega+4j-3m^2-6\omega^2+2i\omega-2\right)+3am(2\omega+i)\\
&-3\omega(\omega+i)\Big)+a^2\cos^6\theta\Big(a^4\left(12j^2-18ij\omega-17j-6\omega^2+15i\omega+7\right)+3a^3m(6ij+4\omega-5i)\\
&+a^2\left(-18ij\omega+2j-6m^2-12\omega^2+13i\omega+5\right)+2am(6\omega+i)-6\omega^2-2i\omega+8\Big)\\
&+\cos^4\theta\Big(a^4\left(18j^2+j(-17-18i\omega)-3\omega^2+11i\omega-1\right)+a^3m(18ij+6\omega-11i)\\
&-a^2\left(2j(4+9i\omega)+3m^2+6\omega^2-12i\omega+10\right)+am(6\omega-i)+(-3\omega+i)\omega\Big)\\
&+3j^2+5j+1\Big],
\end{aligned}
\tag{E.10}
$$

$$
d_5(\theta) = \frac{\sqrt{1+a^2}\cos\theta^2\sin^2\theta}{(1+a^2)\,(1+a^2\cos^2\theta)},
\tag{E.11}
$$

$$
d_6(\theta) = \frac{\cos\theta\sin\theta\left(\cos^2\theta\left(a^2(j-i\omega-2)+iam-i\omega\right)+j-1\right)}{\sqrt{1+a^2}\,(1+a^2\cos^2\theta)}.
\tag{E.12}
$$

The coefficients $c_6(\theta)$ and $d_4(\theta)$ have very lengthy forms. They are written as

$$
c_6(\theta) = \frac{1}{(a^2+1)^4\cos^3\theta\,(1+a^2\cos^2\theta)^2}\sum_{k=0}^{k=7}\hat{c}_6^{(k)}\cos^{2k}\theta,
\tag{E.13}
$$

and

$$
d_4(\theta) = \frac{1}{(1+a^2)^2\cos^2\theta\,(1+a^2\cos^2\theta)^4}\sum_{k=0}^{k=6}\hat{d}_4^{k}\cos^{2k}\theta,
\tag{E.14}
$$

where

$$
\hat{c}_6^{(0)} = j\left(j^2+8j+12\right),
\tag{E.15}
$$

$$
\begin{aligned}
\hat{c}_6^{(1)} = &\,j\Big(a^2\left(5j^2-3ij\omega+23j-10i\omega+16\right)\\
&+ia(3j+10)m-j^2-3ij(\omega-5i)-10i\omega-28\Big),
\end{aligned}
\tag{E.16}
$$

$$
\begin{aligned}
\hat{c}_6^{(2)} = &\,a^4\left(10j^3+j^2(18-13i\omega)-j\left(3\omega^2+19i\omega+8\right)-2\left(\omega^2-2i\omega+4\right)\right)\\
&+a^3m\left(13ij^2+6j\omega+19ij+4\omega-4i\right)-a^2\Big(5j^3+5j^2(9+2i\omega)\\
&+j\left(3m^2+6\omega^2+44\right)+2\left(m^2+2\omega^2-2i\omega+4\right)\Big)+am\left(-2ij^2+j(6\omega-17i)+4\omega\right)\\
&+j^2(7+3i\omega)+j\left(-3\omega^2+19i\omega+20\right)-2\omega^2,
\end{aligned}
\tag{E.17}
$$

JHEP09(2015)193

$$\begin{aligned}\hat{c}_6^{(3)} &= a^6\left(10j^3+j^2(-4-22i\omega)-j\left(11\omega^2+14\right)+i\left(\omega^3+8\omega+8i\right)\right)\\&+a^5m\left(22ij^2+22j\omega-i\left(3\omega^2+8\right)\right)+a^4\Big(-10j^3+j^2(-42-9i\omega)\\&+j\left(-11m^2+(-19\omega+39i)\omega\right)+i\left(3m^2+4\right)\omega+3i\omega^3+4\omega^2+8\Big)\\&-ia^3m\left(8j^2+2j(19+9i\omega)+m^2+6\omega^2-8i\omega-4\right)+a^2\Big(j^2(22+13i\omega)\\&+j\left(m^2-5\omega^2+30i\omega+34\right)+m^2(4+3i\omega)+3i\omega^3+8\omega^2-4i\omega+16\Big)\\&-am(j(4\omega-6i)+(8+3i\omega)\omega)+3j\omega^2-9ij\omega-4j+i\omega^3+4\omega^2, \qquad \text{(E.18)}\\ \hat{c}_6^{(4)} &= a^8\left(5j^3+j^2(-10-18i\omega)-3j\omega(5\omega-6i)+3i\omega^3+7\omega^2+8\right)\\&+a^7m\left(18ij^2+6j(5\omega-3i)+(-14-9i\omega)\omega\right)+a^6\Big(-10j^3+j^2(-6+4i\omega)\\&+j\left(-15m^2-19\omega^2+28i\omega+18\right)+m^2(7+9i\omega)+8i\omega^3+15\omega^2-10i\omega+32\Big)\\&-ia^5m\left(12j^2+4j(5+4i\omega)+3m^2+16\omega^2-21i\omega-12\right)+a^4\Big(j^2(24+22i\omega)\\&+j\left(3m^2+7\omega^2-10i\omega+8\right)+m^2(6+8i\omega)+6i\omega^3+7\omega^2-12i\omega+16\Big)\\&-a^3m(14j(\omega-i)+(4+5i\omega)\omega)+a^2\Big(j\left(11\omega^2-20i\omega-6\right)+m^2(-1-i\omega)\\&-3\omega^2-2i\omega-8\Big)+am(3+2i\omega)\omega+(-2-i\omega)\omega^2, \qquad \text{(E.19)}\\ \hat{c}_6^{(5)} &= a^2\Bigg(a^8\left(j^3+j^2(-3-7i\omega)+j\left(-9\omega^2+10i\omega+2\right)+\omega\left(3i\omega^2+6\omega-4i\right)\right)\\&+a^7m\left(7ij^2+2j(9\omega-5i)-i(-3\omega+2i)^2\right)+a^6\Big(-5j^3+j^2(9+11i\omega)\\&-3j\left(3m^2+\omega(\omega+4i)\right)+m^2(6+9i\omega)+6i\omega^3+\omega^2-4i\omega-8\Big)\\&-ia^5m\left(8j^2-6j+3m^2+12\omega^2-i\omega-4\right)+a^4\Big(2j^2(5+9i\omega)\\&+j\left(3m^2+21\omega^2-32i\omega-6\right)+2i\left(3m^2-1\right)\omega-17\omega^2-24\Big)\\&+a^3m\left(-2j(9\omega-5i)+3i\omega^2+14\omega-4i\right)+a^2\Big(5j(3\omega-2i)\omega+m^2(-2-3i\omega)\\&-6i\omega^3-13\omega^2-16\Big)+3am(1+2i\omega)\omega+\omega\left(-3i\omega^2-\omega+2i\right)\Bigg), \qquad \text{(E.20)}\\ \hat{c}_6^{(6)} &= a^4\Bigg(a^8\omega\left(-ij^2-2j\omega+ij+i\omega^2+\omega\right)+a^7m\left(ij^2+j(4\omega-i)+(-2-3i\omega)\omega\right)\\&+a^6\left(-j^3+j^2(3+6i\omega)-j\left(2m^2-5\omega^2+12i\omega+2\right)+m^2(1+3i\omega)+(-7\omega+6i)\omega\right)\\&-ia^5m\left(2j^2+j(-5-6i\omega)+m^2+9i\omega+4\right)+a^4\Big(j^2(1+7i\omega)+j\left(m^2+\omega(16\omega-9i)\right)\\&-2m^2+\omega\left(-6i\omega^2-13\omega+4i\right)\Big)+a^3m\left(j(-10\omega+2i)+9i\omega^2+8\omega-4i\right)\\&+a^2\left(j\left(9\omega^2+4i\omega+2\right)+m^2(-1-3i\omega)+\omega\left(-8i\omega^2-\omega+2i\right)\right)\\&+3iam\omega(2\omega+i)+\omega\left(-3i\omega^2+4\omega+4i\right)\Bigg), \qquad \text{(E.21)}\end{aligned}$$

JHEP09(2015)193

$$\hat{c}_6^{(7)} = a^6\left(a^2+1\right)\omega\Big(a^4\left(ij^2+j(2\omega-i)+(-1-i\omega)\omega\right)+a^3m(-2j+2i\omega+1)$$
$$+a^2\left(j(2\omega+3i)-i\left(m^2+2\omega^2+2i\omega+2\right)\right)+am(-3+2i\omega)$$
$$-i\omega^2+3\omega+2i\Big), \tag{E.22}$$
$$\hat{d}_4^{(0)} = -j(j+2)^2, \tag{E.23}$$
$$\hat{d}_4^{(1)} = j\Big(a^2\left(-6j^2+j(-11+3i\omega)+2i\omega-8\right)-ia(3j+2)m$$
$$+j(5+3i\omega)+2i\omega+8\Big), \tag{E.24}$$
$$\hat{d}_4^{(2)} = a^4\left(-15j^3+j^2(-3+15i\omega)+j\left(3\omega^2-5i\omega+2\right)-2\left(\omega^2-2i\omega+4\right)\right)$$
$$+a^3m\left(-15ij^2-6j\omega+5ij+4\omega-4i\right)+a^2\Big(j^2(17+15i\omega)+j\left(3m^2+6\omega^2-10i\omega+26\right)$$
$$-2\left(m^2+2\omega^2-2i\omega+4\right)\Big)+am(4\omega+j(-6\omega+5i))+j\left(3\omega^2-5i\omega-4\right)-2\omega^2, \tag{E.25}$$
$$\hat{d}_4^{(3)} = a^6\left(-20j^3+6j^2(3+5i\omega)+2j\left(6\omega^2-15i\omega+5\right)-i\omega\left(\omega^2-10i\omega-4\right)\right)$$
$$+a^5m\left(-30ij^2-6j(4\omega-5i)+3i\omega^2+20\omega-4i\right)+a^4\Big(6j^2(3+5i\omega)$$
$$+4j\left(3m^2+6\omega^2-10i\omega+6\right)+m^2(-10-3i\omega)-3i\omega^3-20\omega^2-8i\omega+16\Big)$$
$$+a^3m\left(j(-24\omega+10i)+i\left(m^2+6\omega^2-20i\omega+12\right)\right)+a^2\Big(2j\left(6\omega^2-5i\omega-9\right)$$
$$-3i\left(m^2+4\right)\omega-3i\omega^3-10\omega^2+16\Big)+3iam\omega^2-i\omega^3, \tag{E.26}$$
$$\hat{d}_4^{(4)} = -a^2\Bigg(a^6\left(15j^3+j^2(-22-30i\omega)-2j\left(9\omega^2-20i\omega+1\right)+3i\omega^3+16\omega^2-4i\omega+8\right)$$
$$+a^5m\left(30ij^2+4j(9\omega-10i)-9i\omega^2-32\omega+4i\right)+a^4\Big(j^2(-2-30i\omega)$$
$$-2j\left(9m^2+18\omega^2-20i\omega+2\right)+m^2(16+9i\omega)+9i\omega^3+30\omega^2+8i\omega+16\Big)$$
$$-a^3m\left(-36j\omega+3im^2+18i\omega^2+28\omega+12i\right)+a^2\Big(j\left(26-18\omega^2\right)+m^2(-2+9i\omega)$$
$$+9i\omega^3+12\omega^2+4i\omega+16\Big)+am\left(-9i\omega^2+4\omega+8i\right)+3i\omega^3-2\omega^2-8i\omega+8\Bigg), \tag{E.27}$$
$$\hat{d}_4^{(5)} = a^4\Bigg(a^6\left(-6j^3+3j^2(3+5i\omega)+2j\left(6\omega^2-10i\omega-1\right)+\omega\left(-3i\omega^2-10\omega+4i\right)\right)$$
$$+a^5m\left(-15ij^2-4j(6\omega-5i)+9i\omega^2+20\omega-4i\right)+a^4\Big(j^2(-7+15i\omega)$$
$$+2j\left(6m^2+\omega(12\omega-5i)\right)+m^2(-10-9i\omega)-9i\omega^3-16\omega^2+8\Big)$$
$$+a^3m\left(-2j(12\omega+5i)+3im^2+18i\omega^2+12\omega+4i\right)+a^2\Big(2j\left(6\omega^2+5i\omega-7\right)$$
$$+m^2(4-9i\omega)-9i\omega^3-2\omega^2+4i\omega+16\Big)+iam\left(9\omega^2+8i\omega-8\right)$$
$$-3i\omega^3+4\omega^2+8i\omega+8\Bigg), \tag{E.28}$$

JHEP09(2015)193

$$\hat{d}_4^{(6)} = -a^6\Bigg(a^6\left(j^3+j^2(-1-3i\omega)-3j\omega(\omega-i)+(2+i\omega)\omega^2\right)$$
$$+a^5m\left(3ij^2+j(6\omega-3i)+(-4-3i\omega)\omega\right)+a^4\Big(j^2(3-3i\omega)$$
$$-j\left(3m^2+6\omega^2+2i\omega+2\right)+m^2(2+3i\omega)+\omega\left(3i\omega^2+2\omega+4i\right)\Big)$$
$$-ia^3m\left(j(-5+6i\omega)+m^2+6\omega^2+4\right)+a^2\Big(j\left(-3\omega^2-5i\omega+2\right)$$
$$+i\left(m^2(3\omega+2i)+\omega\left(3\omega^2+2i\omega+4\right)\right)\Big)+am(4-3i\omega)\omega+i\omega^2(\omega+2i)\Bigg). \tag{E.29}$$

F Explicit form of δ_ω^S

The QNM condition for the scalar type perturbation of the Myers-Perry black hole is

$$\delta_\omega^S = \ell - j. \tag{F.1}$$

This condition can be rewritten as

$$\delta_\omega^S - \ell + j = 0 \Leftrightarrow \frac{F(\omega)}{G(\omega)} = 0, \tag{F.2}$$

where

$$G(\omega) = \left(1+a^2\right)^3\Big[a^4(j-i\omega)^2+2a^3m(\omega+ij)$$
$$-a^2\left(j(-2\ell+2i\omega+4)+2i\ell\omega+m^2+2\omega^2-4i\omega-4\right)$$
$$+2am(i\ell+\omega-2i)+(\ell-i\omega-2)^2\Big], \tag{F.3}$$

and

$$F(\omega) = f_5\omega^5+f_4\omega^4+f_3\omega^3+f_2\omega^2+f_1\omega+f_0. \tag{F.4}$$

Each coefficient is

$$f0_5 = i\left(1+a^2\right)^5, \tag{F.5}$$
$$f_4 = -\left(1+a^2\right)^4\left(a^2(5j-2)+5iam+5\ell-6\right), \tag{F.6}$$
$$f_3 = -i\left(1+a^2\right)^3\Big(a^4j(10j-7)+4ia^3(5j-2)m+a^2\big(j(20\ell-21)$$
$$-9\ell-10m^2+12\big)+2ia(10\ell-11)m+10\ell^2-23\ell+12\Big), \tag{F.7}$$
$$f_2 = \left(1+a^2\right)^2\Big(a^6j^2(10j-9)+3ia^5j(10j-7)m+a^4\big(3j^2(10\ell-9)$$
$$-6j\left(4\ell+5m^2-5\right)+2\left(\ell+6m^2-4\right)\big)-ia^3m\big(j(57-60\ell)+27\ell$$
$$+10m^2-30\big)+a^2\left(30j(\ell-1)^2-15\ell^2-30\ell m^2+34\ell+30m^2-16\right)$$
$$+3ia\left(10\ell^2-21\ell+10\right)m+10\ell^3-33\ell^2+32\ell-8\Big), \tag{F.8}$$

JHEP09(2015)193

$$
\begin{aligned}
f_1 = i\left(1+a^2\right)\Big(&5a^8(j-1)j^3+2ia^7j^2(10j-9)m+a^6j\big(5j^2(4\ell-3)\\
&-3j\left(7\ell+10m^2-8\right)+4\ell+21m^2-12\big)-4ia^5m\big(-3j^2(5\ell-4)\\
&+j\left(12\ell+5m^2-12\right)-\ell-2m^2+3\big)+a^4\big(3j^2\left(10\ell^2-17\ell+8\right)\\
&+j\left(-27\ell^2+\ell\left(56-60m^2\right)+51m^2-24\right)+4\ell^2+3\ell\left(9m^2-4\right)+m^2\left(5m^2-24\right)\big)\\
&-2ia^3m\left(-6j\left(5\ell^2-9\ell+4\right)+15\ell^2+2\ell\left(5m^2-14\right)-9m^2+12\right)\\
&+a^2\left(j\left(20\ell^3-57\ell^2+52\ell-12\right)-11\ell^3+\ell^2\left(32-30m^2\right)+3\ell\left(19m^2-8\right)-24m^2\right)\\
&+4ia\left(5\ell^3-15\ell^2+13\ell-3\right)m+\ell\left(5\ell^3-21\ell^2+28\ell-12\right)\Big),
\end{aligned}
\tag{F.9}
$$

and

$$
\begin{aligned}
f_0 = -\left(a^2j+iam+\ell\right)^2\Big(&a^6(j-1)j^2+3ia^5(j-1)jm\\
&+a^4\left(3j^2(\ell-1)+j\left(-4\ell-3m^2+6\right)+2\left(\ell+m^2-2\right)\right)\\
&-ia^3m\left(j(7-6\ell)+5\ell+m^2-6\right)+a^2\big(j\left(3\ell^2-8\ell+6\right)-3\ell^2\\
&-3\ell m^2+10\ell+4m^2-8\big)+3ia\left(\ell^2-3\ell+2\right)m+(\ell-2)^2(\ell-1)\Big).
\end{aligned}
\tag{F.10}
$$

References

[1] V. Asnin, D. Gorbonos, S. Hadar, B. Kol, M. Levi and U. Miyamoto, *High and Low Dimensions in The Black Hole Negative Mode*, *Class. Quant. Grav.* **24** (2007) 5527 [arXiv:0706.1555] [INSPIRE].

[2] R. Emparan, R. Suzuki and K. Tanabe, *The large D limit of General Relativity*, *JHEP* **06** (2013) 009 [arXiv:1302.6382] [INSPIRE].

[3] R. Emparan, D. Grumiller and K. Tanabe, *Large-D gravity and low-D strings*, *Phys. Rev. Lett.* **110** (2013) 251102 [arXiv:1303.1995] [INSPIRE].

[4] R. Emparan and K. Tanabe, *Holographic superconductivity in the large D expansion*, *JHEP* **01** (2014) 145 [arXiv:1312.1108] [INSPIRE].

[5] R. Emparan and K. Tanabe, *Universal quasinormal modes of large D black holes*, *Phys. Rev.* **D 89** (2014) 064028 [arXiv:1401.1957] [INSPIRE].

[6] R. Emparan, R. Suzuki and K. Tanabe, *Instability of rotating black holes: large D analysis*, *JHEP* **06** (2014) 106 [arXiv:1402.6215] [INSPIRE].

[7] R. Emparan, R. Suzuki and K. Tanabe, *Decoupling and non-decoupling dynamics of large D black holes*, *JHEP* **07** (2014) 113 [arXiv:1406.1258] [INSPIRE].

[8] R. Emparan, R. Suzuki and K. Tanabe, *Quasinormal modes of (Anti-)de Sitter black holes in the 1/D expansion*, *JHEP* **04** (2015) 085 [arXiv:1502.02820] [INSPIRE].

[9] R. Emparan, T. Shiromizu, R. Suzuki, K. Tanabe and T. Tanaka, *Effective theory of Black Holes in the 1/D expansion*, *JHEP* **06** (2015) 159 [arXiv:1504.06489] [INSPIRE].

JHEP09(2015)193

[10] S. Bhattacharyya, A. De, S. Minwalla, R. Mohan and A. Saha, *A membrane paradigm at large D*, arXiv:1504.06613 [INSPIRE].

[11] T. Damour, *Surface Effects in Black Hole Physics*, Proceedings of the *Second Marcel Grossmann Meeting on General Relativity*, R. Ruffni ed., North Holland, (1982) pg. 587.

[12] R.H. Price and K.S. Thorne, *Membrane Viewpoint on Black Holes: Properties and Evolution of the Stretched Horizon*, *Phys. Rev.* **D 33** (1986) 915 [INSPIRE].

[13] R. Emparan, T. Harmark, V. Niarchos and N.A. Obers, *Essentials of Blackfold Dynamics*, *JHEP* **03** (2010) 063 [arXiv:0910.1601] [INSPIRE].

[14] R.C. Myers and M.J. Perry, *Black Holes in Higher Dimensional Space-Times*, *Annals Phys.* **172** (1986) 304 [INSPIRE].

[15] S.W. Hawking, C.J. Hunter and M. Taylor, *Rotation and the AdS/CFT correspondence*, *Phys. Rev.* **D 59** (1999) 064005 [hep-th/9811056] [INSPIRE].

[16] G.W. Gibbons, H. Lü, D.N. Page and C.N. Pope, *The General Kerr-de Sitter metrics in all dimensions*, *J. Geom. Phys.* **53** (2005) 49 [hep-th/0404008] [INSPIRE].

[17] O.J.C. Dias, J.E. Santos and B. Way, *Rings, Ripples and Rotation: Connecting Black Holes to Black Rings*, *JHEP* **07** (2014) 045 [arXiv:1402.6345] [INSPIRE].

[18] R. Emparan, P. Figueras and M. Martinez, *Bumpy black holes*, *JHEP* **12** (2014) 072 [arXiv:1410.4764] [INSPIRE].

[19] B. Kleihaus, J. Kunz and E. Radu, *Black rings in six dimensions*, *Phys. Lett.* **B 718** (2013) 1073 [arXiv:1205.5437] [INSPIRE].

[20] J.M. Bardeen, B. Carter and S.W. Hawking, *The four laws of black hole mechanics*, *Commun. Math. Phys.* **31** (1973) 161 [INSPIRE].

[21] M.M. Caldarelli, O.J.C. Dias, R. Emparan and D. Klemm, *Black Holes as Lumps of Fluid*, *JHEP* **04** (2009) 024 [arXiv:0811.2381] [INSPIRE].

[22] W. Hsiang, Z. Teng and W. Yu, *Examples of constant mean curvature immersions of the 3-sphere into euclidean 4-space*, *Proc. Natl. Acad. Sci. USA* **79** (1982) 3931.

[23] G.W. Gibbons, D. Ida and T. Shiromizu, *Uniqueness and nonuniqueness of static black holes in higher dimensions*, *Phys. Rev. Lett.* **89** (2002) 041101 [hep-th/0206049] [INSPIRE].

[24] R. Emparan and R.C. Myers, *Instability of ultra-spinning black holes*, *JHEP* **09** (2003) 025 [hep-th/0308056] [INSPIRE].

[25] O.J.C. Dias, P. Figueras, R. Monteiro, J.E. Santos and R. Emparan, *Instability and new phases of higher-dimensional rotating black holes*, *Phys. Rev.* **D 80** (2009) 111701 [arXiv:0907.2248] [INSPIRE].

[26] O.J.C. Dias, P. Figueras, R. Monteiro and J.E. Santos, *Ultraspinning instability of rotating black holes*, *Phys. Rev.* **D 82** (2010) 104025 [arXiv:1006.1904] [INSPIRE].

[27] H. Kodama and A. Ishibashi, *A master equation for gravitational perturbations of maximally symmetric black holes in higher dimensions*, *Prog. Theor. Phys.* **110** (2003) 701 [hep-th/0305147] [INSPIRE].

[28] D. Gorbonos and B. Kol, *A dialogue of multipoles: Matched asymptotic expansion for caged black holes*, *JHEP* **06** (2004) 053 [hep-th/0406002] [INSPIRE].

JHEP09(2015)193

[29] . J.C. Dias, G.S. Hartnett and J.E. Santos, *Quasinormal modes of asymptotically flat rotating black holes*, *Class. Quant. Grav.* **31** (2014) 245011 [arXiv:1402.7047] [INSPIRE].

[30] H. Kodama and A. Ishibashi, *Master equations for perturbations of generalized static black holes with charge in higher dimensions*, *Prog. Theor. Phys.* **111** (2004) 29 [hep-th/0308128] [INSPIRE].

[31] H. Kodama, R.A. Konoplya and A. Zhidenko, *Gravitational stability of simply rotating Myers-Perry black holes: Tensorial perturbations*, *Phys. Rev.* **D 81** (2010) 044007 [arXiv:0904.2154] [INSPIRE].

[32] R. Gregory and R. Laflamme, *Black strings and p-branes are unstable*, *Phys. Rev. Lett.* **70** (1993) 2837 [hep-th/9301052] [INSPIRE].

[33] H. Kudoh, *Origin of black string instability*, *Phys. Rev.* **D 73** (2006) 104034 [hep-th/0602001] [INSPIRE].

[34] G.S. Hartnett and J.E. Santos, *Non-Axisymmetric Instability of Rotating Black Holes in Higher Dimensions*, *Phys. Rev.* **D 88** (2013) 041505 [arXiv:1306.4318] [INSPIRE].

[35] M. Shibata and H. Yoshino, *Bar-mode instability of rapidly spinning black hole in higher dimensions: Numerical simulation in general relativity*, *Phys. Rev.* **D 81** (2010) 104035 [arXiv:1004.4970] [INSPIRE].

[36] R. Suzuki and K. Tanabe, *Non-uniform black strings and the critical dimension in the* $1/D$ *expansion*, arXiv:1506.01890 [INSPIRE].

[37] E. Berti, V. Cardoso and M. Casals, *Eigenvalues and eigenfunctions of spin-weighted spheroidal harmonics in four and higher dimensions*, *Phys. Rev.* **D 73** (2006) 024013 [*Erratum ibid.* **D 73** (2006) 109902] [gr-qc/0511111] [INSPIRE].

JHEP09(2015)193